NUREG/CR-4554
UCID-20674
Vol. 3, Rev. 1

SCANS (Shipping Cask ANalysis System) A Microcomputer Based Analysis System for Shipping Cask Design Review

Theory Manual (Lead Slump in Impact Analysis and Verification of Impact Analysis)

Prepared by
R. C. Chun, T. Lo, G. C. Mok, M. C. Witte

Lawrence Livermore National Laboratory

Prepared for
U.S. Nuclear Regulatory Commission

AVAILABILITY NOTICE

Availability of Reference Materials Cited in NRC Publications

Most documents cited in NRC publications will be available from one of the following sources:

1. The NRC Public Document Room, 2120 L Street, NW., Lower Level, Washington, DC 20555
2. The Superintendent of Documents, U.S. Government Printing Office, P.O. Box 37082, Washington, DC 20013-7082
3. The National Technical Information Service, Springfield, VA 22161

Although the listing that follows represents the majority of documents cited in NRC publications, it is not intended to be exhaustive.

Referenced documents available for inspection and copying for a fee from the NRC Public Document Room include NRC correspondence and internal NRC memoranda; NRC bulletins, circulars, information notices, inspection and investigation notices; licensee event reports; vendor reports and correspondence; Commission papers; and applicant and licensee documents and correspondence.

The following documents in the NUREG series are available for purchase from the GPO Sales Program: formal NRC staff and contractor reports, NRC-sponsored conference proceedings, international agreement reports, grant publications, and NRC booklets and brochures. Also available are regulatory guides, NRC regulations in the *Code of Federal Regulations*, and *Nuclear Regulatory Commission Issuances*.

Documents available from the National Technical Information Service include NUREG-series reports and technical reports prepared by other Federal agencies and reports prepared by the Atomic Energy Commission, forerunner agency to the Nuclear Regulatory Commission.

Documents available from public and special technical libraries include all open literature items, such as books, journal articles, and transactions. *Federal Register* notices, Federal and State legislation, and congressional reports can usually be obtained from these libraries.

Documents such as theses, dissertations, foreign reports and translations, and non-NRC conference proceedings are available for purchase from the organization sponsoring the publication cited.

Single copies of NRC draft reports are available free, to the extent of supply, upon written request to the Office of Administration, Distribution and Mail Services Section, U.S. Nuclear Regulatory Commission, Washington, DC 20555.

Copies of industry codes and standards used in a substantive manner in the NRC regulatory process are maintained at the NRC Library, 7920 Norfolk Avenue, Bethesda, Maryland, for use by the public. Codes and standards are usually copyrighted and may be purchased from the originating organization or, if they are American National Standards, from the American National Standards Institute, 1430 Broadway, New York, NY 10018.

NUREG/CR-4554
UCID-20674
Vol. 3, Rev. 1

SCANS (Shipping Cask ANalysis System) A Microcomputer Based Analysis System for Shipping Cask Design Review

Theory Manual (Lead Slump in Impact Analysis and Verification of Impact Analysis)

Manuscript Completed: June 1991
Date Published: February 1992

Prepared by
R. C. Chun, T. Lo, G. C. Mok, M. C. Witte

Lawrence Livermore National Laboratory
7000 East Avenue
Livermore, CA 94550

Prepared for
Division of Safeguards and Transportation
Office of Nuclear Material Safety and Safeguards
U.S. Nuclear Regulatory Commission
Washington, DC 20555
NRC FIN A0291

ABSTRACT

A computer system called SCANS (Shipping Cask ANalysis System) has been developed for the staff of the U.S. Nuclear Regulatory Commission to perform confirmatory licensing review analyses. SCANS can handle problems associated with impact, heat transfer, thermal stress, and pressure. A new methodology was developed to allow SCANS to analyze the lead slump behavior of lead-shielded casks during a postulated impact with an unyielding surface.

The methodology is an expansion of the existing lumped-parameter impact analysis method. In the new methodology, it is assumed that the lead and the steel cylinders are not bonded as opposed to the existing bonded-lead assumption. The lead shield is allowed to slide freely relative to the steel cylinders and interact with the steel cylinders only in the radial direction of the shipping cask.

The interface pressure between the lead and the steel, the hoop stress in the steel shells, and the reduction in shielding are among items that can be calculated. The adequacy of this lead slump methodology is established by comparing results with those obtained from rigorous finite element analyses and from cask impact tests.

The lead slump methodology described in this revision (Rev. 1) of the report is an improved version of the method documented in the original report. The main improvement is in the modeling of the lead behavior. To minimize mathematical difficulty and development cost, the lead was formerly treated as an elastic material with an effective modulus which was tuned to account for the effect of plastic deformation occurring in a cask drop. Although this method gave satisfactory results for 30-ft accident drops, it produced overconservative predictions for 1- to 4-ft normal drops. Thus, the present revision of the method was undertaken to improve the range of applicability of the method. In the improved method described in this report, the lead is treated as an elastic-plastic material and the actual elastic-plastic properties of lead are used instead.

TABLE OF CONTENTS

TABLE OF CONTENTS (con't)

LIST OF FIGURES

LIST OF TABLES

FOREWORD

Lawrence Livermore National Laboratory has developed a system of computer programs to analyze radioactive-material shipping casks. This system is called SCANS (Shipping Cask ANalysis System) and is developed on an IBM-PC microcomputer for use by the staff of the U.S. Nuclear Regulatory Commission to perform confirmatory analyses in their licensing review. In its current version, SCANS can handle problems associated with impact, heat transfer, thermal stress, and pressure. This report documents a newly developed methodology which can assess the effects of lead slump of a lead-shielded shipping cask during impact with an unyielding horizontal surface.

ACKNOWLEDGMENTS

The authors wish to thank C. R. Chappell and H. W. Lee, technical monitors at the U.S. Nuclear Regulatory Commission, for their support and technical direction. The authors also thank Professor R. L. Taylor of University of California, Berkeley, and Dr. G. L. Goudreau of Lawrence Livermore National Laboratory (LLNL) for their helpful consultations. Several other LLNL personnel also contributed to this work: D. J. Trummer and M. A. Gerhard, incorporating the CRAY version of the IMPASC code into SCANS; D. L. Paquette, K. Wood, and D. Sceales, editing; and J. L. Prince, M. A. Carter, S. Wilson, and S. Murray, word processing.

EXECUTIVE SUMMARY

Lawrence Livermore National Laboratory, under contract to the U.S. Nuclear Regulatory Commission (NRC), has developed a system of computer programs called Shipping Cask ANalysis System (SCANS) for the NRC staff to perform confirmatory licensing review analyses. In its current version, SCANS can handle problems associated with impact, heat transfer, thermal stress, and pressure. This report documents a newly developed methodology which, having been fully implemented in SCANS, can assess lead slump behavior of lead-shielded casks during impact with an essentially unyielding horizontal surface. Also presented in this report are verification results for this lead slump analysis method and for SCANS' impact analysis capabilities.

The methodology is an expansion of the existing impact analysis method and consists of two parts:

(1) The first part is essentially the same as the existing dynamic lumped-parameter impact analysis, and is used to simulate the overall behavior of the cask. In this part of the impact analysis, complete bonding between steel and lead is assumed because the lead slump is believed to have insignificant effect on the overall behavior of the cask. The locations and corresponding accelerations of lumped masses are calculated in this part of the impact analysis.

(2) The lead-steel interaction is a local behavior and is studied in the second part of the impact analysis. In this analysis, no bonding between the lead and the steel cylinders is assumed. The lead and steel shells can slide freely relative to each other.

In the first part of analysis, linear elastic behavior of the lead and the steel is assumed. However, for the second analysis the lead is treated as an elastic-plastic medium.

In the lead slump analysis, kinematic relationships between the lead and the steel shells in the radial and hoop directions are first established. The equilibrium equations and the stress-strain relationships of the lead and the steel are then formulated. By a series of complicated manipulations of these equations, the axial stresses of the lead and the steel can be expressed as functions of axial strains. As in the case of impact analysis without lead slump, the equations of motion can be solved by the central difference method.

The interface pressure between the lead and the steel, the hoop stress in the steel shells, and the amount of shielding reduction at the opposite end of impact can be calculated in addition to all other results available in the existing impact analysis without lead slump.

The lead slump methodology developed here for SCANS is a simplified approach. However, as shown in this report, the method can produce results that compare closely with those of a more sophisticated finite element computer program, NIKE. The amount of shielding reduction or permanent lead slump predicted by the method also agrees with the results of an Oak Ridge test.

SCANS (Shipping Cask ANalysis System)
Volume 3--Theory Manual
Lead Slump in Impact Analysis and Verification of Impact Analysis*

1.0 INTRODUCTION

1.1 Background

Lawrence Livermore National Laboratory has developed a system of computer programs to analyze spent fuel shipping casks. This system is called SCANS (Shipping Cask ANalysis System) and is developed on an IBM-PC microcomputer. SCANS is intended for use by the staff of the U.S. Nuclear Regulatory Commission to perform licensing-related confirmatory analyses. In its current version, SCANS can handle problems associated with impact, heat transfer, thermal stress, and pressure. Typical configuration of a laminated cask for various analyses using SCANS is shown in Fig. 1-1.

The impact portion of SCANS is composed of two computer modules, IMPASC (IMPact Analysis of Shipping Containers) and QUASC (QUasi-static Analysis of Shipping Containers). IMPASC (Refs. 1 and 2) is based on the dynamic lumped-parameter method and is an explicit finite-element computer code. IMPASC includes one type of element—the beam element. The mass of the cask is lumped at element ends and the beam element is assumed to have no mass. The cask is modeled as an elastic composite material, but the impact limiter can have nonlinear force-deflection curves. The impact limiter is not explicitly modeled in IMPASC as finite elements, but is in the form of force-deflection curves simulating various possible initial cask impact angles with the horizontal surface.

The other SCANS module, QUASC (Ref. 2), is based on a quasi-static method of impact analysis. QUASC treats casks as slender rigid beams in estimating the maximum impact force and the associated "g" load during impact. Use of QUASC is not always recommended because of its simplifying assumptions described in Ref. 2 and in Chapter 6 of this report.

A third method of impact analysis is the dynamic finite element analysis. Because this method, which is most useful for the analysis of detailed dynamic response, usually requires many accurate finite elements and the use of a mainframe computer, it is not implemented in SCANS. The lumped-parameter method described above, which is sometimes considered to be a simplified finite element approach, uses only a few elements. The dynamic finite element method and the two impact analysis methods included in SCANS are described in detail in Refs. 1 and 2. These impact analysis methods can be summarized in a flow chart as shown in Fig. 1-2.

In the case of a lead-shielded cask with lead laminated between two concentric steel shells, a perfect bonding between the lead in-fill and the steel shells of the cask is assumed in the current version of IMPASC and QUASC. While this assumption is quite reasonable for calculating the overall behavior of the cask during impact, the bonding may not be strong enough to prevent the movement of the lead relative to the steel shells. For convenience, we will use the term "lead slump" to represent the behavior of lead movement relative to steel shells.

---

*This work was supported by the United States Nuclear Regulatory Commission under a Memorandum of Understanding with the United States Department of Energy.

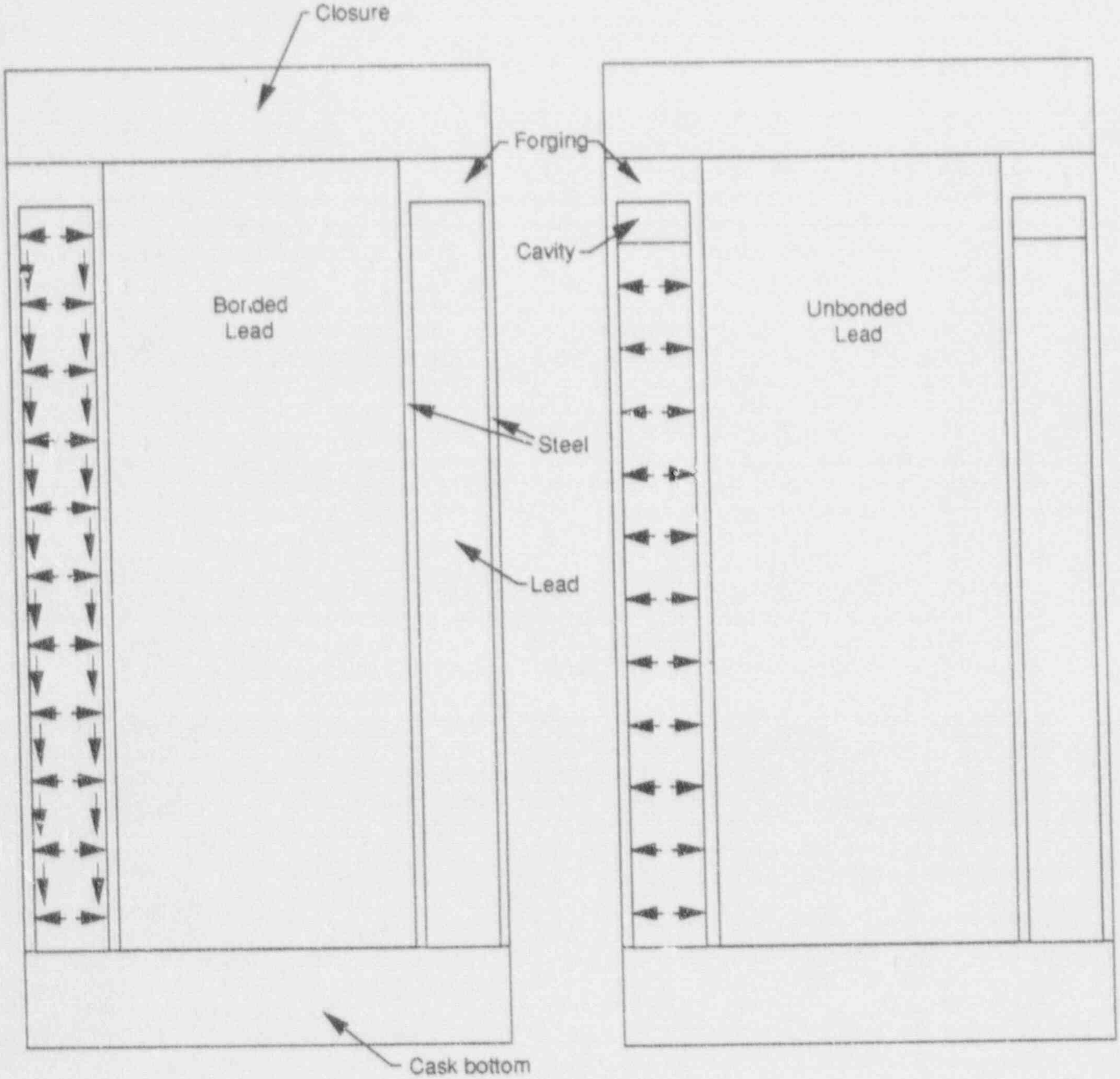

Figure 1-1 A typical laminated Shipping Cask and illustration of lead slump.

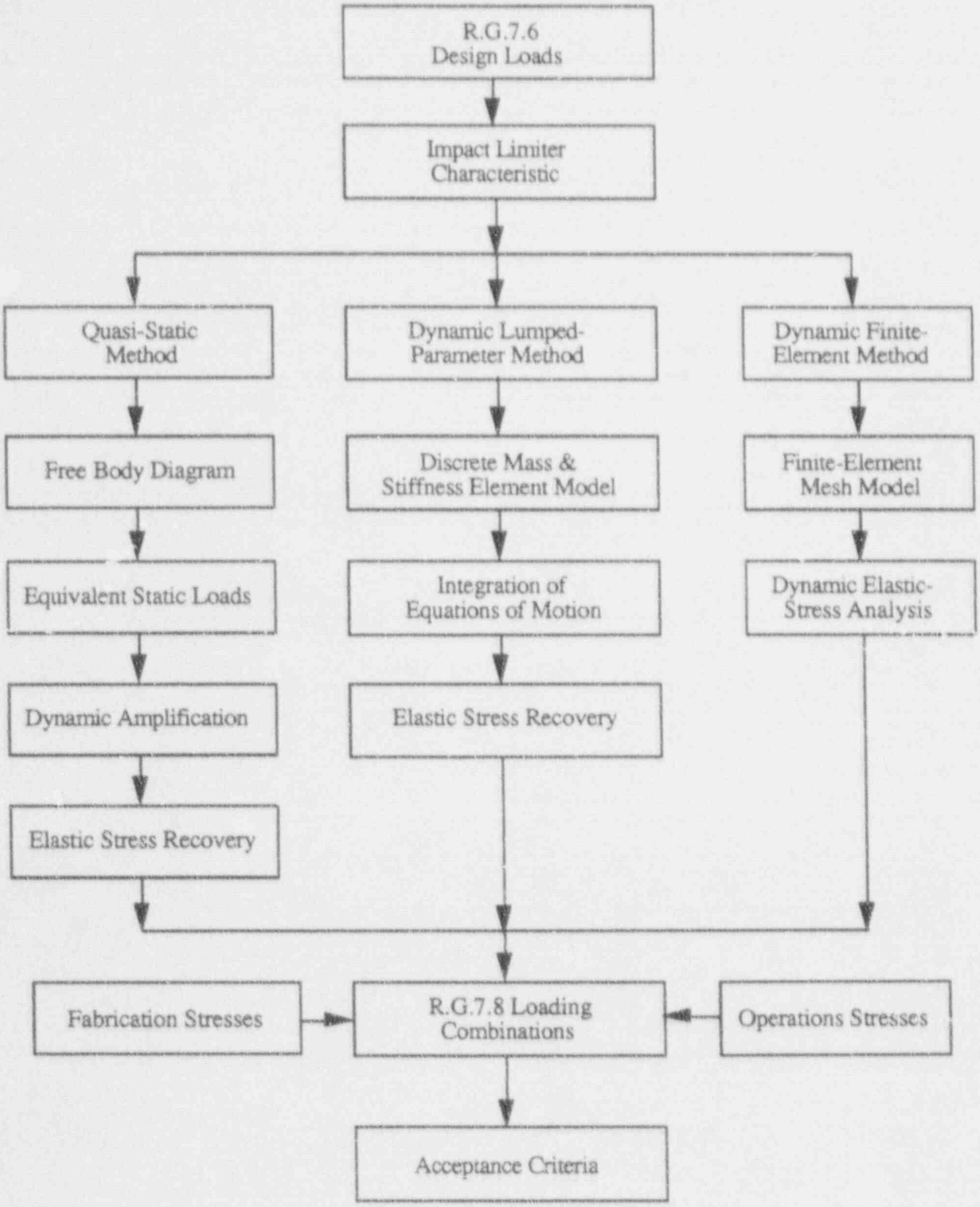

Figure 1-2 Impact analysis of a spent fuel shipping cask.

Two effects of lead slump are of interest in the design of spent fuel shipping casks. Severe lead slump in the axial direction will result in a cavity at the opposite end of impact. This cavity will reduce effectiveness of the shielding function of the lead. The other effect is the hoop stress in the steel shells caused by the interface pressure between the lead and the steel shells during lead slump. Large hoop stress is objectionable because of possible material failure or buckling of steel shells.

1.2 OBJECTIVE

A task under the framework of SCANS was started in 1986. The objective was to develop a lead slump methodology for analyzing shipping casks with laminated cylindrical side walls. This methodology will be applicable not only to the lead but also to any other shielding materials. This lead slump methodology and the current impact analysis methods in which lead and steel are assumed bonded provide the bounding cases of lead behavior for evaluating shipping casks. The result of the lead slump analysis can be used to assess the integrity of the containment system of spent fuel casks by evaluating the stress level and the buckling potential of steel shells. The work on developing a buckling analysis capability in SCANS is documented in Vol. 6 of the theory manual.

This report documents the lead slump work associated with unbonded lead, which has been implemented in both the IMPASC and QUASC modules of SCANS. The output information includes shell stresses (including hoop stress) and interface pressure due to lead slump during impact.

The lead slump methodology developed here is a simplified method for confirmatory analysis. It is not intended to replace finite element analysis in calculating local stresses of a shipping cask.

2.0 GENERAL DESCRIPTION OF THE METHOD OF ANALYSIS

The lead slump methodology reported here is developed under the framework of impact analysis methods of the existing SCANS. We are expanding the methodology implemented in the existing IMPASC and QUASC modules to include lead slump effects. The basic principle and formulation of lead slump for the two modules are identical. Therefore, we will detail the implementation of this method only in the IMPASC module. Readers are urged to become familiar with the existing dynamic lumped-parameter method documented in Ref. 1 because the method of handling large rigid-body rotation and the explicit method of integration remain unchanged.

We believe that the amount of lead slump has insignificant effect on the spatial motion (overall behavior) of the cask. The existing impact analysis of bonded lead can still be used to calculate the spatial locations of lumped mass points of a finite-element model.

The effects of lead slump, a local phenomenon, can be handled separately but concurrently with the impact analysis. In the following section (Section 2.1), we will briefly review the impact analysis. The lead slump analysis, or local impact analysis, will be described briefly in Section 2.2 and in greater detail in the remaining chapters of this report.

2.1 Impact Analysis of a Cask with Bonded-Lead Assumption

The impact analysis of a shipping cask without considering lead slump is documented in Ref. 1. The equation of motion has the following form:

$$[M]\{\ddot{X}\} = \{F\} - \{P\}\ , \tag{2-1}$$

where [M] is the mass matrix of the lumped mass dynamic analysis model, {P} is the internal force vector of finite elements, and {F} is the external force vectors acting on lumped masses. The external force includes the gravitational force and the reaction force of the impact limiter. There are three degrees of freedom at each lumped mass point. A dynamic analysis model with three lumped mass points is shown in Fig. 2-1 to illustrate various parts of Eq. (2-1). For a dynamic analysis model with n lumped masses, [M], {X}, {P}, and {F} can be expressed as shown in Fig. 2-2.

For a typical beam element k, shown in Fig. 2-3, the internal force vector $\{p^k\}$ has six components, three at each end of the beam element:

$$\{p^k\} = \begin{Bmatrix} p^k_{ix} \\ p^k_{iy} \\ p^k_{i\theta} \\ p^k_{jx} \\ p^k_{jy} \\ p^k_{j\theta} \end{Bmatrix}\ . \tag{2-2}$$

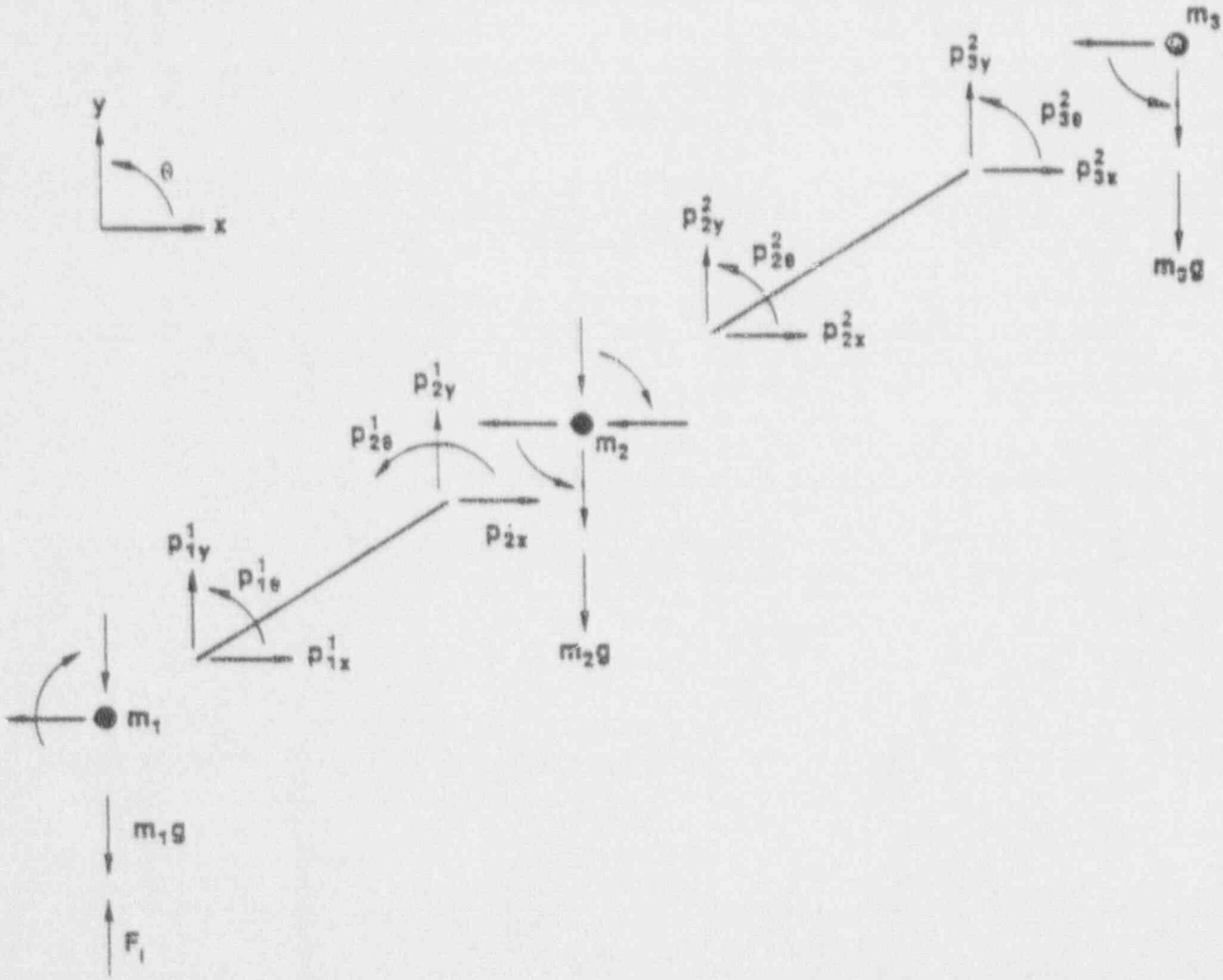

x = horizontal degree of freedom
y = vertical degree of freedom
θ = rotational degree of freedom
p^k_{ij} = internal force of k^{th} element in j direction at lumped mass point i.
m_i = lumped mass at node i
F_i = reaction force of impact limiter

Figure 2-1 Free body diagram of a three-mass lumped-parameter model.

$$
M = \begin{bmatrix} m_1 & & & & & & & & & \\ & m_1 & & & & & & & 0 & \\ & & I_1 & & & & & & & \\ & & & m_2 & & & & & & \\ & & & & m_2 & & & & & \\ & & & & & I_2 & & & & \\ & & & & & & \ddots & & & \\ & 0 & & & & & & m_n & & \\ & & & & & & & & m_n & \\ & & & & & & & & & I_n \end{bmatrix}
\qquad
x = \begin{Bmatrix} x_1 \\ y_1 \\ \theta_1 \\ x_2 \\ y_2 \\ \theta_2 \\ \vdots \\ x_n \\ y_n \\ \theta_n \end{Bmatrix}
$$

$$
F = \begin{Bmatrix} 0 \\ F_1 - m_1 g \\ 0 \\ 0 \\ -m_2 g \\ 0 \\ \vdots \\ 0 \\ -m_n g \\ 0 \end{Bmatrix}
\qquad
-P = \begin{Bmatrix} -P^1_{1x} \\ -P^1_{1y} \\ -P^1_{1\theta} \\ -P^1_{2x} - P^2_{2x} \\ -P^1_{2y} - P^2_{2y} \\ -P^1_{2\theta} - P^2_{2\theta} \\ \vdots \\ -P^{n-1}_{nx} \\ -P^{n-1}_{ny} \\ -P^{n-1}_{n\theta} \end{Bmatrix}
$$

Figure 2-2 Elements of the equation of motion.

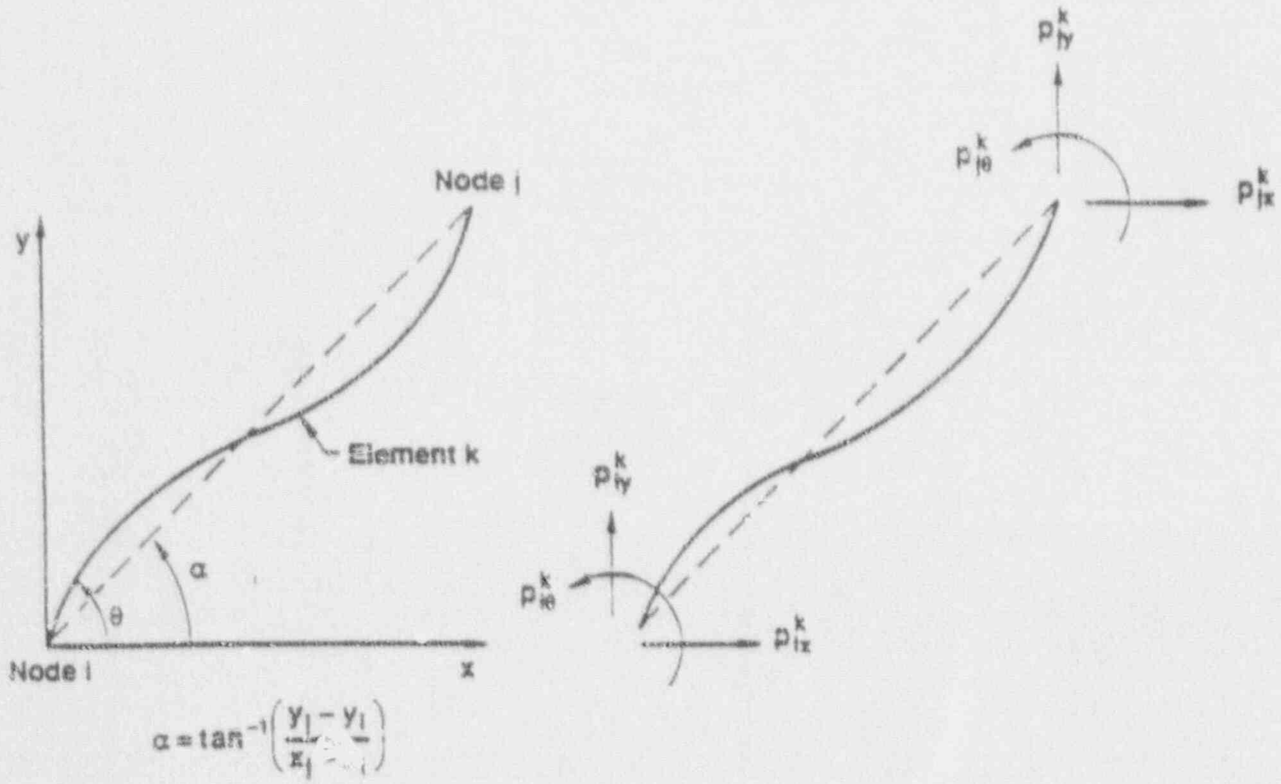

Figure 2-3 Free body diagram of a beam element in global coordinates.

The notations are shown in Fig. 2-1. These six components of $\{p^k\}$ can be expressed in terms of four components of the generalized forces of the beam element in local coordinates (Fig. 2-4):

$$\{p^k\} = \begin{Bmatrix} -R\cos\alpha - V\sin\alpha \\ -R\sin\alpha + V\cos\alpha \\ M_i \\ R\cos\alpha + V\sin\alpha \\ R\sin\alpha - V\cos\alpha \\ M_j \end{Bmatrix} . \qquad (2\text{-}3)$$

In the above formulation, R is the axial force, V is the shear force, and M_i and M_j are the end moments of the beam element. These generalized forces R, V, M_i, and M_j can be calculated using the following formulae (Ref. 3):

$$R = AE(L - L_o)/L_o , \qquad (2\text{-}4)$$

$$\begin{Bmatrix} M_i \\ M_j \end{Bmatrix} = [EI/L(1+\phi)] \begin{bmatrix} 4+\phi & 2-\phi \\ 2-\phi & 4+\phi \end{bmatrix} \begin{Bmatrix} \beta_i \\ \beta_j \end{Bmatrix} , \qquad (2\text{-}5)$$

$$V = (M_i + M_j)/L , \qquad (2\text{-}6)$$

where

- A = the cross-sectional area of the beam,
- E = Young's modulus,
- I = moment of inertia of the beam cross section,
- L_o = original length of the beam element,
- L = current chord length of the beam element,
- β_i = chord deflections at the ends of the beam element,
- ϕ = $12EI/GA_sL^2 = 24(1+\nu)(EI)/EA_sL^2$,
- G = shear modulus
- ν = Poisson's ratio, and
- A_s = effective shear area of the beam cross section.

The impact limiter force-deflection curve is modeled by a piece-wise linear function as shown in Fig. 2-5.

Equation 2-1 can be solved by the method of central difference. This integration method is documented in detail in Ref. 1.

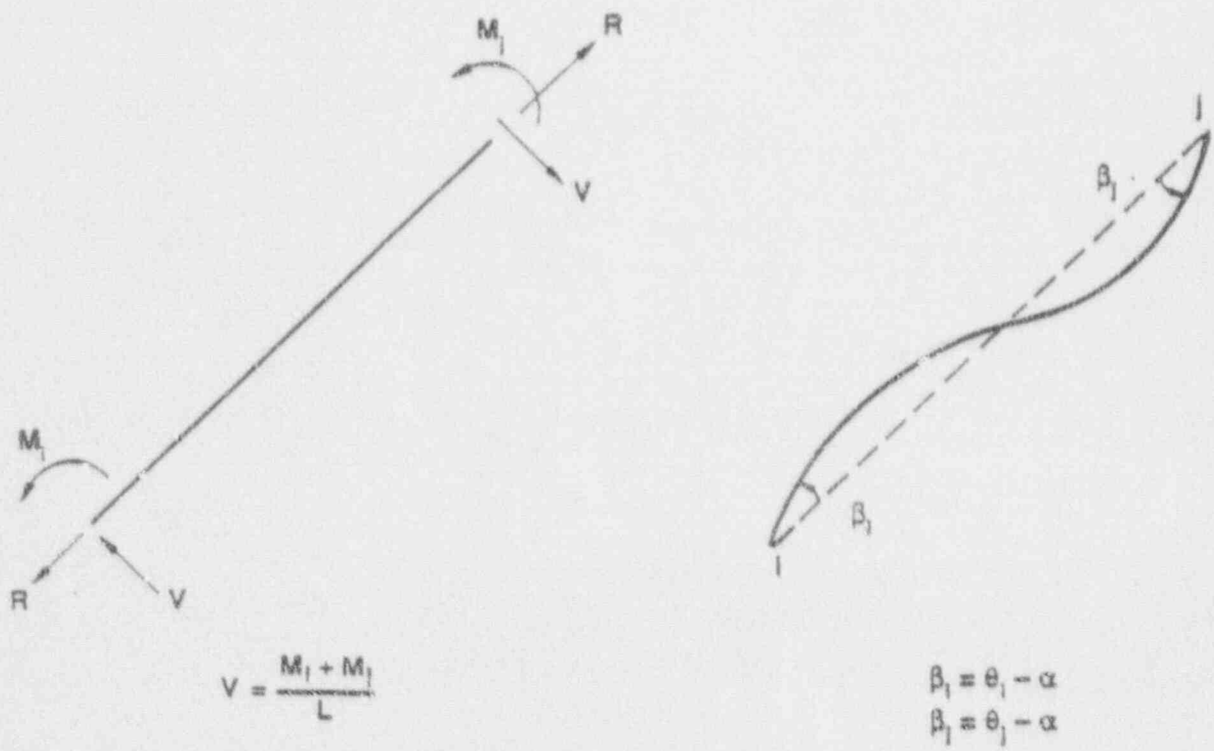

Figure 2-4 Free body diagram of a beam element in local coordinates.

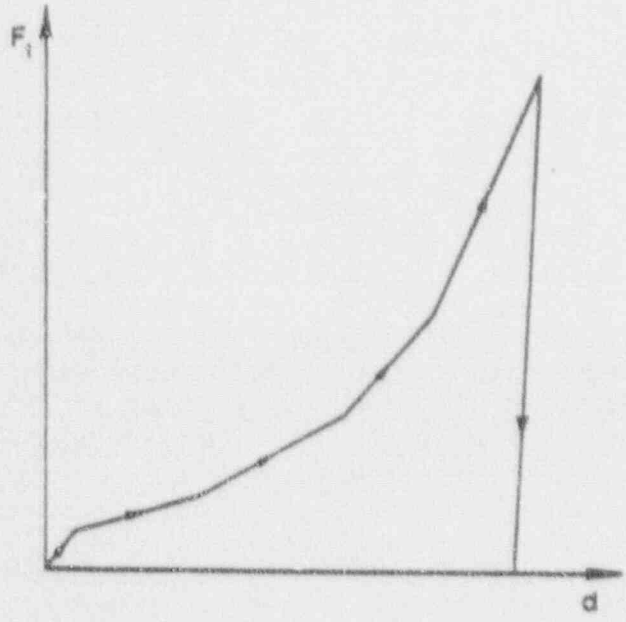

Figure 2-5 Force-deformation relationship of an impact limiter.

2.2 Lead-Steel Interaction

The loading on the cask during an oblique impact can be decomposed into axial and transverse components. End-on impact is a special case of oblique impact in which the transverse component is nil. Side impact is another special case of oblique impact. Bending due to transverse impact load is the dominant mode of failure; and no axial impact load is associated with side impact.

The axial component of loading can cause axial slumping of lead and create a cavity at the opposite end of impact. Loading in the axial direction also causes an interface pressure to develop between the lead and the steel shells due to axisymmetric slumping of the lead.

Compared to the axial component, the transverse impact load will have insignificant effects in terms of cavity and interface pressure creation. A cavity forming between the steel shells and the lead along the length of the cask is extremely unlikely because of the large flexibility of the lead and the steel shells in the transverse direction.

Because the transverse impact load on lead slump is insignificant, it is not considered in calculating the amount of lead slump. Thus, lead slump because of the axial loading component becomes the core of this lead slump methodology. Equations of motion of lead and steel in the axial direction are developed to simulate local lead and steel behavior. These axial equations of motion are in addition to those of impact analysis for bonded lead, which simulate the overall behavior of the cask. The combined equations of motion can be expressed in the following form:

$$\begin{bmatrix} M & o & o \\ o & M^S & o \\ o & o & M^L \end{bmatrix} \begin{Bmatrix} \ddot{X} \\ \ddot{z}^S \\ \ddot{z}^L \end{Bmatrix} + \begin{Bmatrix} P \\ P_z^S \\ P_z^L \end{Bmatrix} = \begin{Bmatrix} F \\ F_z^S \\ F_z^L \end{Bmatrix} , \qquad (2-7)$$

where z is a local axial coordinate which moves along with the global coordinate X of the cask. In other words, X represents the global location of lumped-mass points, and z represents the local deformation of lead and steel shells in the axial direction in studying lead slump effects. The superscripts, S and L, represent steel and lead, respectively. Whereas the axial deformation as calculated in global coordinate X is used to calculate axial stresses, it is replaced by z^S and z^L in calculating impact with lead slump.

To study lead slump in the axial direction, the steel linings of the cask are assumed to be thin elastic shells and the lead is modeled as a linear elastic and work-hardening plastic medium. In this approach, the amount of lead slump is equal to the permanent plastic deformation of the lead column.

Using the equilibrium equations, the kinematics, and the stress-strain laws of steel and lead, the radial and the hoop strains of the lead can be expressed as the axial strains of the lead and the steel. In so doing, the internal force term in the axial equations of motion of lead and steel can be expressed as functions of axial deformations alone by eliminating all radial and hoop strains. The beauty of this mathematical manipulation is that the internal force term can be calculated easily in the central difference method of integration because the axial deformation, which is the integration variable, is the only information needed. The detail of the mathematical derivation is presented in Chapters 3 and 4 of this report.

The major lead slump effects that remain to be addressed are shear stress due to transverse impact force and normal stress due to the bending effect of this transverse force. Because no bonding is assumed between the lead and the steel, the cask needs to be represented by two steel beams and a lead beam constrained to move together in the transverse direction at every point along the full length of the cask. These beams have the same curvature but are allowed to slide relative to each other in the axial direction.

Because these three beams are concentric and have the same neutral axis under bending, points on a plane section cut across these beams before bending will remain on a single plane after bending. Under this situation, these three beams are acting like a single composite beam whether bonded or not. Figure 2-6 further demonstrates the validity of a composite beam approach.

The shear stress distributions on these beams have the same shape. Maximum shear stresses of different values occur at the neutral axis of these beams. However, the beams all have zero shear at the top and the bottom of their respective cross sections. Interface forces develop between the steel shells and the lead due to the transverse impact force. However, these interface forces are small and can be ignored in evaluating lead slump as described earlier in this chapter.

In short, the lead slump problem during impact can be analyzed by considering axial and transverse loads separately. A methodology has been developed to study lead slump effects due to axial impact load. The reduction in shielding at the opposite end of the cask impact will be estimated. The interface pressure between the lead and the steel shells will also be calculated. The effects on lead slump due to transverse impact load will be ignored. In the transverse direction, the cask will be treated as a single composite beam. Tangential (or transverse in-plane) shear stress and normal stress in the steel shells due to bending can be calculated easily.

The effects of lead slump on steel shells will be more severe in an end-on impact than at any other cask orientation. This is because during an end-on impact, the inertial force is in the direction of lead flow. Lead slump in the secondary impact is also expected to be much less severe than in the primary impact. Thus, lead slump analysis for secondary impact will not be included in SCANS.

Details of the lead slump analysis are presented in the following two chapters. Boundary conditions of steel shells are discussed in Chapter 5, and validation of the lead slump methodology is presented in Chapter 6.

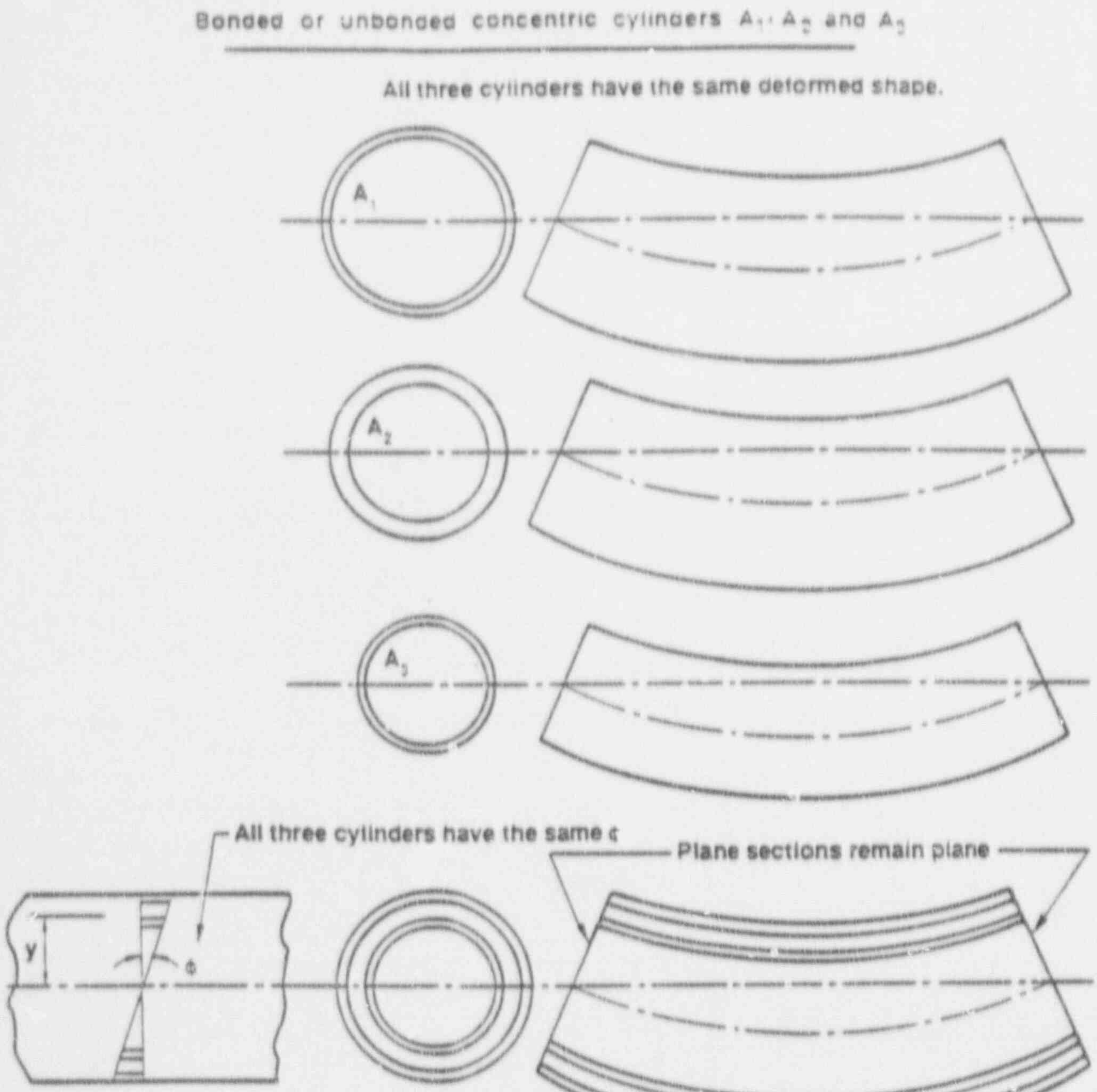

$$M = \int y\,\sigma\,dA = \int_{A_1} y\,\sigma\,dA + \int_{A_2} y\,\sigma\,dA + \int_{A_3} y\,\sigma\,dA$$

$$= E_1\int_{A_1} y^2\,\phi\,dA + E_2\int_{A_2} y^2\,\phi\,dA + E_3\int_{A_3} y^2\,\phi\,dA$$

$$M = (E_1 I_1 + E_2 I_2 + E_3 I_3)\phi = E\,I\,\phi$$

Figure 2-6 Section property of bonded and unbonded composite beams.

3.0 THEORETICAL PREREQUISITES

3.1 Kinematics

3.1.1 Kinematics of Thin Steel Shells

In the lumped-parameter method of impact analysis the cask is divided into finite elements along the cask axis. The primary step in the lead slump analysis is to calculate the axial positions of the steel and lead of individual elements, z^S and z^L, where z is the axial displacement, and the superscripts S and L refer to steel and lead, respectively.

From our basic assumption of equal end displacements of inner and outer shells, we have the following relationship for strains in the axial direction:

$$\varepsilon_z^i = \varepsilon_z^o = \varepsilon_z^S , \quad (3\text{-}1)$$

where the superscripts i and o refer to inner and outer steel shells, respectively, and the subscript z refers to the direction of strain.

Hoop strains of inner and outer steel shells can be found from the displacements in the radial direction, u^i and u^o:

$$\varepsilon_\theta^i = \frac{u^i}{r^i} , \quad (3\text{-}2)$$

$$\varepsilon_\theta^o = \frac{u^o}{r^o} . \quad (3\text{-}3)$$

The radial strain is not zero, but can be condensed out in a thin shell theory. See Section 3.3.2 for details. The axial strain is just the ratio of the change of the axial length to the original length of the steel shells.

3.1.2 Lead Kinematics

The lead is assumed to be an elastic medium. The axial strain can be calculated as the ratio of the change of the axial length to the original length of the lead in a particular element. The strains in radial and hoop directions can be expressed in terms of radial displacements of the inner and outer steel shells, u^i and u^o:

$$\varepsilon_r^L = \frac{du}{dr} = \frac{u^o - u^i}{r^o - r^i} = \frac{u^o - u^i}{t^L} , \quad (3\text{-}4)$$

$$\varepsilon_\theta^L = \frac{u}{r} = \frac{u^o + u^i}{2r^L} , \tag{3-5}$$

where r is the radial position, and t is the thickness of the lead:

$$t^L = r^o - r^i , \tag{3-6}$$

$$r^L = \frac{1}{2}(r^o + r^i) . \tag{3-7}$$

Expressing displacements in terms of strains, the lead kinematic relationships (Eqs. 3-4 and 3-5) can be rewritten as:

$$u^o = r^L \varepsilon_\theta^L + \frac{1}{2} t^L \varepsilon_r^L , \tag{3-8}$$

$$u^i = r^L \varepsilon_\theta^L - \frac{1}{2} t^L \varepsilon_r^L . \tag{3-9}$$

3.1.3 Strain Relationships Between Lead and Steel

Substituting Eqs. 3-8 and 3-9 for Eqs. 3-2 and 3-3, we obtain the relationships between the strains in lead and steel:

$$\varepsilon_\theta^i = \frac{r^L}{r^i} \varepsilon_\theta^L - \frac{1}{2} \frac{t^L}{r^i} \varepsilon_r^L , \tag{3-10}$$

$$\varepsilon_\theta^o = \frac{r^L}{r^o} \varepsilon_\theta^L + \frac{1}{2} \frac{t^L}{r^o} \varepsilon_r^L . \tag{3-11}$$

3.2 Equilibrium Equations

3.2.1 Lead Equilibrium

Consider the equilibrium of a lead element subjected to a virtual displacement in the axial direction:

$$(2\pi r^i h)(p^i)(\delta u^i) + (2\pi r^o h)(p^o)(-\delta u^o) + p_z^L(\delta u_z^T - \delta u_z^B) = \int_V (\sigma_j^L \delta\epsilon_j^L)\, dv\ , \tag{3-12}$$

where

h = length of the lead element,

u_z^T = axial displacement at the top of the lead element,

u_z^B = axial displacement at the bottom of the lead element,

P_z^L = axial force on the lead element,

p^i = pressure on the inside surface of the lead element,

p^o = pressure on the outside surface of the lead element.

Since

$$\delta u_z^T - \delta u_z^B = h\delta\epsilon_z^L\ , \tag{3-13}$$

and from Eqs. 3-8 and 3-9,

$$\delta u^o = r^L\delta\epsilon_\theta^L + \frac{1}{2}\, t^L\delta\epsilon_r^L\ , \tag{3-14}$$

$$\delta u^i = r^L\delta\epsilon_\theta^L - \frac{1}{2}\, t^L\, \delta\epsilon_r^L\ , \tag{3-15}$$

we obtain the following three equations for the lead from Eq. 3-12 because $\delta\epsilon_r^L$, $\delta\epsilon_\theta^L$, and $\delta\epsilon_z^L$ are arbitrary variables:

$$\sigma_r^L = -\frac{(p^i r^i + p^o r^o)}{2r^L} , \quad (3\text{-}16)$$

$$\sigma_\theta^L = \frac{(p^i r^i - p^o r^o)}{t^L} , \quad (3\text{-}17)$$

$$\sigma_z^L = \frac{P_z^L}{A^L} , \quad (3\text{-}18)$$

where A^L is the cross-sectional area of the lead.

3.2.2 Equilibrium of Thin Steel Shells

The following simple equilibrium equations of circular cylinders under external or internal pressure are applicable to the inner and outer steel shells:

$$\sigma_\theta^i = -\frac{p^i r^i}{t^i} , \quad (3\text{-}19)$$

$$\sigma_\theta^o = \frac{p^o r^o}{t^o} . \quad (3\text{-}20)$$

Writing the above equations in another format, we have:

$$p^i = -\frac{t^i}{r^i}\sigma_\theta^i , \quad (3\text{-}21)$$

$$p^o = \frac{t^o}{r^o}\sigma_\theta^o . \quad (3\text{-}22)$$

3.3 Stress-Strain Relationships

As described in Chapter 2, the lead is treated as an elastic-plastic medium. Its stress-strain relationships consist of three parts, namely, a yield condition to determine when the plastic flow appears, and two sets of stress-strain relationships for the elastic and plastic deformations, respectively. For the elastic steel shells, only the elastic relationships are needed. Hooke's law is used for the elastic relationships. The von Mises criterion of yielding is used for the yield condition, and the Prandtl-Reuss flow rule is used as the stress-strain relationships for the plastic deformation (Refs. 10 and 11).

3.3.1 Elastic Stress-Strain Relationships

Generalized Hooke's law for a homogeneous isotopic medium can be written in the following form:

$$s_{ij} = \left(K - \frac{2}{3} G\right)\varepsilon_{aa}\delta_{ij} + 2G\varepsilon_{ij} . \qquad (3\text{-}23)$$

where K and G are the bulk and shear moduli of the material, respectively. K and G are related to the Young's modulus E and the Poisson's ratio ν of the material through the following relationships:

$$K = \frac{E}{3(1-2\nu)} , \qquad (3\text{-}24)$$

$$G = \frac{E}{2(1+\nu)} . \qquad (3\text{-}25)$$

Applying Eq. 3-23 to the lead of the cask, we have the following elastic stress-strain relationships for lead:

$$\sigma_r^L = \left[\frac{E_L(1-\nu_L)}{(1+\nu_L)(1-2\nu_L)}\right]\varepsilon_r^L + \nu_L\left[\frac{E_L}{(1+\nu_L)(1-2\nu_L)}\right]\varepsilon_\theta^L + \nu_L\left[\frac{E_L}{(1+\nu_L)(1-2\nu_L)}\right]\varepsilon_z^L , \qquad (3\text{-}26)$$

$$\sigma_\theta^L = \nu_L\left[\frac{E_L}{(1+\nu_L)(1-2\nu_L)}\right]\varepsilon_r^L + \left[\frac{E_L(1-\nu_L)}{(1+\nu_L)(1-2\nu_L)}\right]\varepsilon_\theta^L + \nu_L\left[\frac{E_L}{(1+\nu_L)(1-2\nu_L)}\right]\varepsilon_z^L , \qquad (3\text{-}27)$$

$$\sigma_z^L = \nu_L\left[\frac{E_L}{(1+\nu_L)(1-2\nu_L)}\right]\varepsilon_r^L + \nu_L\left[\frac{E_L}{(1+\nu_L)(1-2\nu_L)}\right]\varepsilon_\theta^L + \left[\frac{E_L(1-\nu_L)}{(1+\nu_L)(1-2\nu_L)}\right]\varepsilon_z^L , \qquad (3\text{-}28)$$

where the subscript and superscript L denotes quantities of the lead.

The same stress-strain relationships (Eq. 3-26 through 3-28) are applicable to both the inner and outer cylinders.

Since the steel cylinders are assumed to be thin shells, the radial stress is equal to zero. By condensing out the radial strain, ε_r, in the equations, we obtain the following equations for either inner or outer shells:

$$\sigma_\theta^i = \left(\frac{E_i}{1-\nu_i^2}\right)\varepsilon_\theta^i + \nu_i\left(\frac{E_i}{1-\nu_i^2}\right)\varepsilon_z^i \ , \tag{3-29}$$

$$\sigma_z^i = \nu_i\left(\frac{E_i}{1-\nu_i^2}\right)\varepsilon_\theta^i + \left(\frac{E_i}{1-\nu_i^2}\right)\varepsilon_z^i \ , \tag{3-30}$$

where the subscript and superscript i denote quantities of the inner shell.

3.3.2 Yield Condition of Lead

Applying the von Mises criterion of yielding, the yield condition of lead can be written as follows:

$$(\sigma_z^L - \sigma_r^L)^2 + (\sigma_r^L - \sigma_\theta^L)^2 + (\sigma_\theta^L - \sigma_z^L)^2 = 2(\bar{\sigma}^L)^2 \ , \tag{3-31}$$

where $\bar{\sigma}^L$ is the equivalent stress, which is related to the equivalent plastic strain $\bar{\varepsilon}_p^L$; i.e.,

$$\bar{\sigma}^L = H\,(\bar{\varepsilon}_p^L) \ . \tag{3-32}$$

The same function H also relates the axial stress to the axial plastic strain in the results of a simple tension test. For the present analysis, an exponential function is used; i.e.,

$$\bar{\sigma}^L = \sigma_o\,(\bar{\varepsilon}_p^L)^m + \sigma_p^L \ , \tag{3-33}$$

where σ_p^L is the proportional stress limit; σ_o and m are constants determined by curve fitting available stress-strain curves from simple tension or compression test. The σ_p^L, σ_o, and m values used in SCANS for lead shield are 250 psi, 8500 psi, and 0.503, respectively. Figure 3-1 compares this lead stress-strain curve of SCANS to some published curves (Refs. 6 through 11). The published data shows a considerable amount of scatter which is attributable to more than a few effects. However, the dominant effect appears to be of the strain rate. The data show a general trend that at a given strain higher stresses are associated with higher strain rates. The stress-strain curves at higher stress levels are from impact tests, while the curves at lower stress levels are from quasi-static tests. Figure 3-1 also shows that the SCANS stress-strain curve is located between these two sets of data from impact and static tests. Thus using the SCANS curve for lead slump analysis will produce predictions more conservative than using the impact data but not as conservative as using the static data.

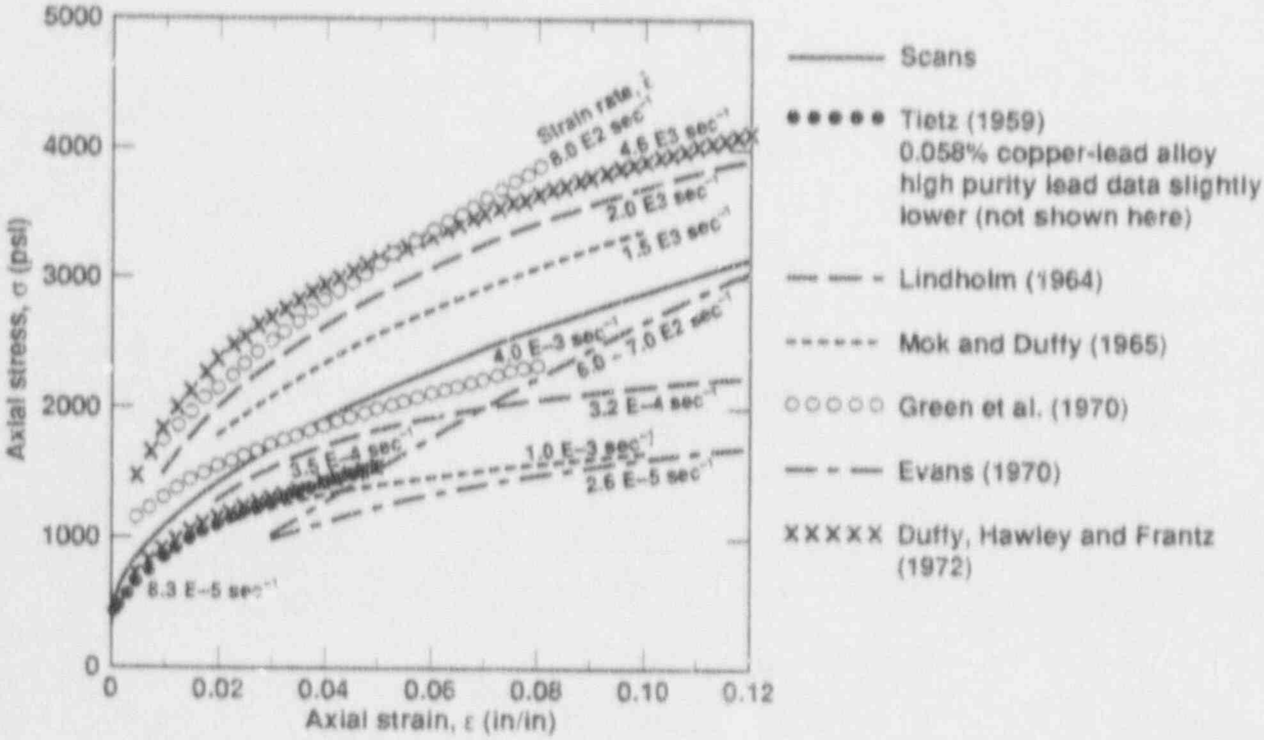

Figure 3-1 Stress-strain curves of lead (comparison of SCANS to published test results).

3.3.3 Plastic Stress-Strain Relationships of Lead

In the plastic range, a strain increment $d\varepsilon$ of lead is composed of an elastic component, $(d\varepsilon)_e$, and a plastic components, $(d\varepsilon)_p$. Using Hooke's law for the stress-strain relationship of the elastic deformation and the Prandtl-Reuss flow rule for the relationship of the plastic deformation, the elastic-plastic stress-strain relationships for lead can be written as follows:

$$\frac{1}{E_L} d\sigma_r^L - \frac{\nu_L}{E_L} d\sigma_\theta^L - \frac{\nu_L}{E_L} d\sigma_z^L + \frac{3S_r^L}{2\bar{\sigma}^L} d\bar{\varepsilon}_p^L = d\varepsilon_r^L \ , \qquad (3\text{-}34)$$

$$-\frac{\nu_L}{E_L} d\sigma_r^L + \frac{1}{E_L} d\sigma_\theta^L - \frac{\nu_L}{E_L} d\sigma_z^L + \frac{3S_\theta^L}{2\bar{\sigma}^L} d\bar{\varepsilon}_p^L = d\varepsilon_\theta^L \ , \qquad (3\text{-}35)$$

$$-\frac{\nu_L}{E_L} d\sigma_r^L - \frac{\nu_L}{E_L} d\sigma_\theta^L + \frac{1}{E_L} d\sigma_z^L + \frac{3S_z^L}{2\bar{\sigma}^L} d\bar{\varepsilon}_p^L = d\varepsilon_z^L \ , \qquad (3\text{-}36)$$

where S_r^L, S_θ^L, and S_z^L are deviatoric stresses. A deviatoric stress is defined as the difference between a normal stress and the mean hydrostatic stress; e.g.,

$$S_r^L = \sigma_r^L - \frac{1}{3}(\sigma_r^L + \sigma_\theta^L + \sigma_z^L). \qquad (3\text{-}37)$$

As shown in Refs. 12 and 13, if the yield condition (Eq. 3-31) is rewritten in an implicit differential form, it can be combined with the elastic-plastic stress-strain relationships (Eqs. 3-34 through 3-36) to form a set of symmetrical linear matrix equations:

$$\begin{bmatrix} \frac{1}{E_L} & -\frac{\nu_L}{E_L} & -\frac{\nu_L}{E_L} & \frac{3S_r^L}{2\bar{\sigma}^L} \\ -\frac{\nu_L}{E_L} & \frac{1}{E_L} & -\frac{\nu_L}{E_L} & \frac{3S_\theta^L}{2\bar{\sigma}^L} \\ -\frac{\nu_L}{E_L} & -\frac{\nu_L}{E_L} & \frac{1}{E_L} & \frac{3S_z^L}{2\bar{\sigma}^L} \\ \frac{3S_r^L}{2\bar{\sigma}^L} & \frac{3S_\theta^L}{2\bar{\sigma}^L} & \frac{3S_z^L}{2\bar{\sigma}^L} & -H' \end{bmatrix} \begin{bmatrix} d\sigma_r^L \\ d\sigma_\theta^L \\ d\sigma_z^L \\ d\bar{\varepsilon}_p^L \end{bmatrix} = \begin{bmatrix} d\varepsilon_r^L \\ d\varepsilon_\theta^L \\ d\varepsilon_z^L \\ 0 \end{bmatrix} . \qquad \begin{matrix} (3\text{-}38) \\ (3\text{-}39) \\ (3\text{-}40) \\ (3\text{-}41) \end{matrix}$$

This set of equations can be solved and rewritten into a form similar to Eqs. 3-26 through 3-28 for the elastic stress-strain relationships:

$$d\sigma_r^L = b_{11}\, d\varepsilon_r^L + b_{12}\, d\varepsilon_\theta^L + b_{13} d\varepsilon_z^L \ , \qquad (3\text{-}42)$$

$$d\sigma_\theta^L = b_{21}\, d\varepsilon_r^L + b_{22}\, d\varepsilon_\theta^L + b_{23} d\varepsilon_z^L \ , \qquad (3\text{-}43)$$

$$d\sigma_z^L = b_{31}\, d\varepsilon_r^L + b_{32}\, d\varepsilon_\theta^L + b_{33} d\varepsilon_z^L \ , \qquad (3\text{-}44)$$

$$d\bar{\varepsilon}_p^L = b_{41}\, d\varepsilon_r^L + b_{42} d\varepsilon_\theta^L + b_{43} d\varepsilon_z^L \ , \qquad (3\text{-}45)$$

where the coefficients b_{11} through b_{43} are elements of matrix **B**, which is the inverse of the coefficient matrix of Eqs. 3-38 through 3-41. Equations 3-42 through 3-44 for elastic-plastic deformation are equivalent to Eqs. 3-26 through 3-28 for purely elastic deformation. The coefficients of the elastic equations are constants, but those of the elastic plastic equations vary with the state of stress and thus require re-evaluation for different load levels.

4.0 FORMULATION AND ANALYSIS OF LEAD SLUMP

Chapter 3 describes all the equations governing the radial coupling of the axial lumped-mass models of the lead shield and steel cask shells. These equations can be solved with the axial equations of motion of the models to evaluate the lead slump effect. Since the solution involves plastic deformation, it must be carried out in terms of small increments of the variables involved. The solution procedure used here follows the technique developed by Marcal in Refs. 12 and 13, which the reader may refer to for information on the theoretical basis of the method. The present report is only concerned with the application of the method to the present lead slump problem. This chapter describes the major steps of this procedure and the equations used. To simplify this description, the resulting equations are only qualitatively described in functional form, and the increment of the variables used for the solution are simply represented by the variables themselves.

Just as with the bonded lead, the equations of motion of cask impact involving lead slump can be expressed in a general form:

$$[M]\{\ddot{X}\} = \{F\} - \{P\} .$$

To solve these equations of motion by the central difference method, the internal and external force vectors {P} and {F} must be calculated at every time step. The external forces can be handled the same as without lead slump. For a free drop of a spent fuel cask, the external force includes the gravitational force and the reaction force due to the deformed impact limiter. The internal force is the force acting on the beam elements of the dynamic lumped-mass model. At a lumped-mass point, the internal force vector {P} is the vector sum of element forces at that location. Details of the central difference method are presented in Ref. 1 and will not be elaborated here.

The major task in the impact analysis with lead slump is the formulation of the internal force vector {P}, which will be discussed in the following section (Section 4.1). The equations of motion in the axial direction are presented in Section 4.2. Section 4.3 describes solution procedure and the back-substitutions that are needed to solve the equations and recover various stresses and strains.

4.1 Element Internal Stresses or Forces

4.1.1 Expression of Radial and Hoop Strains of Lead in Terms of Axial Strains

The first step in calculating internal forces is to express radial and hoop strains of lead in terms of axial strains of both steel and lead. This is done in a series of substitutions of the equations presented in Chapter 3.

Equation 3-1 (lead equilibrium equation) can be expressed as:

$$\sigma_r^L = f_1(p^i, p^o) . \qquad (4\text{-}1)$$

(Note: Throughout the rest of this report, the "f's" will mean "function of.")

Substituting p^i and p^o of the equilibrium equations of steel shells (Eqs.3-21 and 3-22) in the above equation, we have:

$$\sigma_r^L = f_2(\sigma_\theta^i, \sigma_\theta^o) . \qquad (4\text{--}2)$$

Substituting the hoop stresses of the steel stress-strain relations (Eq.3-29) in the above equation for the inner and outer shells, we obtain:

$$\sigma_r^L = f_3(\varepsilon_\theta^i, \varepsilon_\theta^o, \varepsilon_z^S) . \qquad (4\text{--}3)$$

After substituting the hoop strains from the kinematic Eqs. 3-10 and 3-11, Eq. 4-3 becomes:

$$\sigma_r^L = f_4(\varepsilon_r^L , \varepsilon_\theta^L , \varepsilon_z^S) . \qquad (4\text{--}4)$$

Through the same process, the hoop stress in lead can be obtained:

$$\sigma_\theta^L = f_5(\varepsilon_r^L , \varepsilon_\theta^L , \varepsilon_z^S) . \qquad (4\text{--}5)$$

Assuming the stress condition in the lead to be within the yield limit, equating the left-hand sides of Eqs. 3-26 and 4-4, and Eqs. 3-27 and 4-5, will yield two equations with variables ε_r^L, ε_θ^L, ε_z^L, and ε_z^S. Thus, we can solve these two equations simultaneously to obtain:

$$\varepsilon_r^L = f_{6e}(\varepsilon_z^L , \varepsilon_z^S) , \qquad (4\text{--}6)$$

$$\varepsilon_\theta^L = f_{7e}(\varepsilon_z^L , \varepsilon_z^S) , \qquad (4\text{--}7)$$

where the subscript e indicates that these equations hold only for elastic deformation. Similar equations can be derived for elastic-plastic deformation. Using Eqs. 3-42 and 3-43 in lieu of Eqs. 3-26 and 3-27, respectively, and repeating the foregoing operation will produce the following set of equations for elastic-plastic deformations:

$$\varepsilon_r^L = f_{6p} (\varepsilon_z^L , \varepsilon_z^S) , \qquad (4\text{--}8)$$

$$\varepsilon_\theta^L = f_{7p} (\varepsilon_z^L , \varepsilon_z^S) , \qquad (4\text{--}9)$$

where the subscript p denotes that the equations are for elastic-plastic deformation. Like the coefficients b_{11}, etc., in Eqs. 3-26 and 3-27, f_{6p} and f_{7p} are stress dependent and must be reevaluated for different stress conditions.

4.1.2 Axial Stress and Axial Force in Lead

Using Eqs. 3-28, 4-6, and 4-7, the axial stress in lead can be expressed as a function of axial strain in lead and steel for the case of pure elastic deformation:

$$\sigma_z^L = f_{8e}(\varepsilon_z^L , \varepsilon_z^S) . \qquad (4\text{-}10)$$

For elastic-plastic deformation, using Eq. 3-44, 4-6, and 4-7 will result in a different equation; i.e.,

$$\sigma_z^L = f_{8p} (\varepsilon_z^L , \varepsilon_z^S) . \qquad (4\text{-}11)$$

Thus, the axial force in lead, P_z^L is as follows:

$$P_z^L = A^L \sigma_z^L = f_{9e}(\varepsilon_z^L , \varepsilon_z^S) , \qquad (4\text{-}12)$$

or

$$P_z^L = A^L \sigma_z^L = f_{9p} (\varepsilon_z^L , \varepsilon_z^S) , \qquad (4\text{-}13)$$

where A^L is the cross-sectional area of lead. Again, the function f_{9p} is stress dependent.

4.1.3 Axial Stress and Axial Force in Steel Shells

From Eq. 3-29, the axial stress in the inner steel shell can be written as:

$$\sigma_z^i = f_{10}(\varepsilon_\theta^i , \varepsilon_z^S) . \qquad (4\text{-}14)$$

After substituting the steel hoop strain of the kinematic equations (Eq. 3-10) in the above, Eq. 4-14 becomes:

$$\sigma_z^i = f_{11}(\varepsilon_r^L , \varepsilon_\theta^L , \varepsilon_z^S) . \qquad (4\text{-}15)$$

Inserting into Eq. 4-15 the expressions of radial and hoop strains in Eqs. 4-6 and 4-7, we obtain:

$$\sigma_z^i = f_{12e}(\varepsilon_z^L , \varepsilon_z^S) . \tag{4-16}$$

The corresponding equation for elastic-plastic case can be obtained using Eqs. 4-8 and 4-10 in lieu of Eqs. 4-6 and 4-7, respectively; i.e.,

$$\sigma_z^i = f_{12p}(\varepsilon_z^L , \varepsilon_z^S) . \tag{4-17}$$

Similarly, we get the axial stress in the outer steel shell:

$$\sigma_z^o = f_{13e}(\varepsilon_z^L , \varepsilon_z^S) , \tag{4-18}$$

$$\sigma_z^o = f_{13p}(\varepsilon_z^L , \varepsilon_z^S) . \tag{4-19}$$

Thus, we obtain the internal force on the steel shells, P_z^S, after considering the areas of inner and outer steel shells, A^i and A^o:

$$P_z^S = A^i\sigma_z^i + A^o \sigma_z^o = f_{14e}(\varepsilon_z^L , \varepsilon_z^S) , \tag{4-20}$$

or

$$P_z^S = f_{14p}(\varepsilon_z^L , \varepsilon_z^S) . \tag{4-21}$$

4.2 Equations of Motion

After the internal forces acting on the lead and the steel are obtained (Eqs. 4-9 and 4-14), we can write the local axial equations of motion for lead and for steel as follows:

$$[M^S]\{\ddot{z}^S\} + \{P_z^S\}(\varepsilon_z^L , \varepsilon_z^S) = \{F_z^S\} , \tag{4-22}$$

$$[M^L]\{\ddot{z}^L\} + \{P_z^L\}(\varepsilon_z^L , \varepsilon_z^S) = \{F_z^L\} , \tag{4-23}$$

where [M] is the mass matrix and {F} is the external force vector. Equations 4-22 and 4-23 can be solved explicitly as discussed in Ref. 1.

As described in Chapter 2, the bonded lead impact analysis is sufficient to characterize the overall behavior of the cask. Therefore, the solutions for bonded lead impact are again obtained at every integration time step of Eqs. 4-15 and 4-16 in lead slump analysis. In other words, the spatial motion of the cask and the associated transverse shear force and bending moment are the same with or without considering lead slump.

The effects of lead slump, which are local compared to the spatial motion of the cask, can be obtained through the integration of Eqs. 4-22 and 4-23. The direct results of the integration are the axial deformations of the lead and steel shells. Other lead slump results, such as the hoop stresses and strains in the steel shells and the interface pressures, can be recovered in a series of back substitutions using formulas presented in this chapter and in Chapter 3.

4.3 Solution and Back-Substitution Procedure

The numerical solution of the lead slump problem using the equations developed in this chapter and Chapter 3 involves the following steps:

1. Evaluate the internal force P and the applied force F for the current time step and form the equations of motion (Eqs. 4-22 and 4-23) for the lead and steel shells.

2. Use the central difference method to convert Eqs. 4-22 and 4-23 into a set of algebraic equations for the calculation of the axial displacements of the lead and steel shells at the next time step from the axial displacements at the current and previous time steps.

3. From the calculated axial displacements, evaluate the change of the axial strains (ε_z^L and ε_z^S) of the lead and steel shells.

4. Assuming elastic deformation, insert the change of axial strains into Eqs. 4-6 and 4-7 to calculate the change of radial and circumferential strains of the lead.

5. Inserting the lead strains into Eqs. 4-4, 4-5, and 4-10, find the change in lead stresses.

6. Use the calculated stresses and the von Mises yield criterion (Eq. 3-31) to determine whether or not the yielding of the lead has occurred.

7. If the lead yields, revise the calculations of Steps 4 and 5, replacing Eqs. 4-6, 4-7, and 4-10 for elastic deformation with corresponding Eqs. 4-8, 4-9, and 4-11 for elastic-plastic deformation. Use the stresses from Step 5 to evaluate the coefficients of the equations for plastic deformation.

8. Insert the new lead stresses from Step 7 into the yield condition (Eq. 3-1) to confirm the plastic state of the lead. Otherwise repeat Steps 4 through 7 until the equations used are consistent with the state of deformation of the lead.

9. Once the stress and strain solution for the lead converges, other results can be obtained as follows:

   - The change of equivalent strain and stress from Eqs. 3-43, 3-32, and 3-33.

   - The axial stress and force of steel shells from Eqs. 4-16 and 4-18 for elastic lead deformation and from Eqs. 4-17 and 4-19 for elastic-plastic deformation.

   - The axial force of the lead from Eqs. 4-12 or 4-13.

10. After the axial forces for the lead and steel shells (P_z^L and P_z^S) are obtained, form the equations of motion (Eqs. 4-22 and 4-23) for the new time step.

11. Repeat the operation of Steps 2 through 10 for each time step until the end of the cask impact.

4.4 Boundary Conditions

One important aspect of the impact analysis with lead slump that was not discussed in the previous section is the boundary conditions at both ends of the cask where the radial displacement of the steel shells is restrained due to the massive cask bottom and upper forging as shown in Fig. 1-1. The following local boundary conditions of the steel shells at one end of top and bottom elements should be met: (1) zero radial displacement; and (2) zero angular rotation relative to the cask axis.

To meet the boundary conditions, the foregoing lead-slump analysis model must be modified to include the effect of non-uniform radial displacement of the steel shells. As depicted in Fig. 4-1, the lead slump model assumes the radial displacement to be uniform within each element, but the displacement can be different for different elements. Thus a discontinuity of radial displacement can exist between two adjoining elements, and the possible effect of this discontinuity is normally small compared to the main effect of lead slump and is ignored in the basic model. To incorporate this secondary effect in the model without effecting a drastic change in the basic assumption and approach of the lead-slump analysis method, an average adjustment or correction to the radial displacement of each element of the lead-slump model is used. The size of this adjustment depends on the discontinuity of radial displacement between the adjoining elements. Since the basic lead slump solution provides an estimate of this discontinuity, its results are used to obtain the necessary displacement adjustment.

To derive the equations for the calculation of the adjustment, formulas given in Ref. 14 are used. The formulas to determine the radial displacement u and the edge rotation ψ of a cylinder when the cylinder is subjected to an edge shear V_o or an edge moment M_o at one end (Fig. 4-2); i.e.,

$$y = -\frac{V_o}{2D\lambda^3} e^{-\lambda x} \cos\lambda x \,, \tag{4-24}$$

$$\psi = \frac{V_o}{2D\lambda^2} e^{-\lambda x} (\cos\lambda x + \sin\lambda x) \,, \tag{4-25}$$

$$y = \frac{M_o}{2D\lambda^2} e^{-\lambda x} (\sin\lambda x - \cos\lambda x) \,, \tag{4-26}$$

$$\psi = \frac{M_o}{D\lambda} e^{-\lambda x} \cos\lambda x \,, \tag{4-27}$$

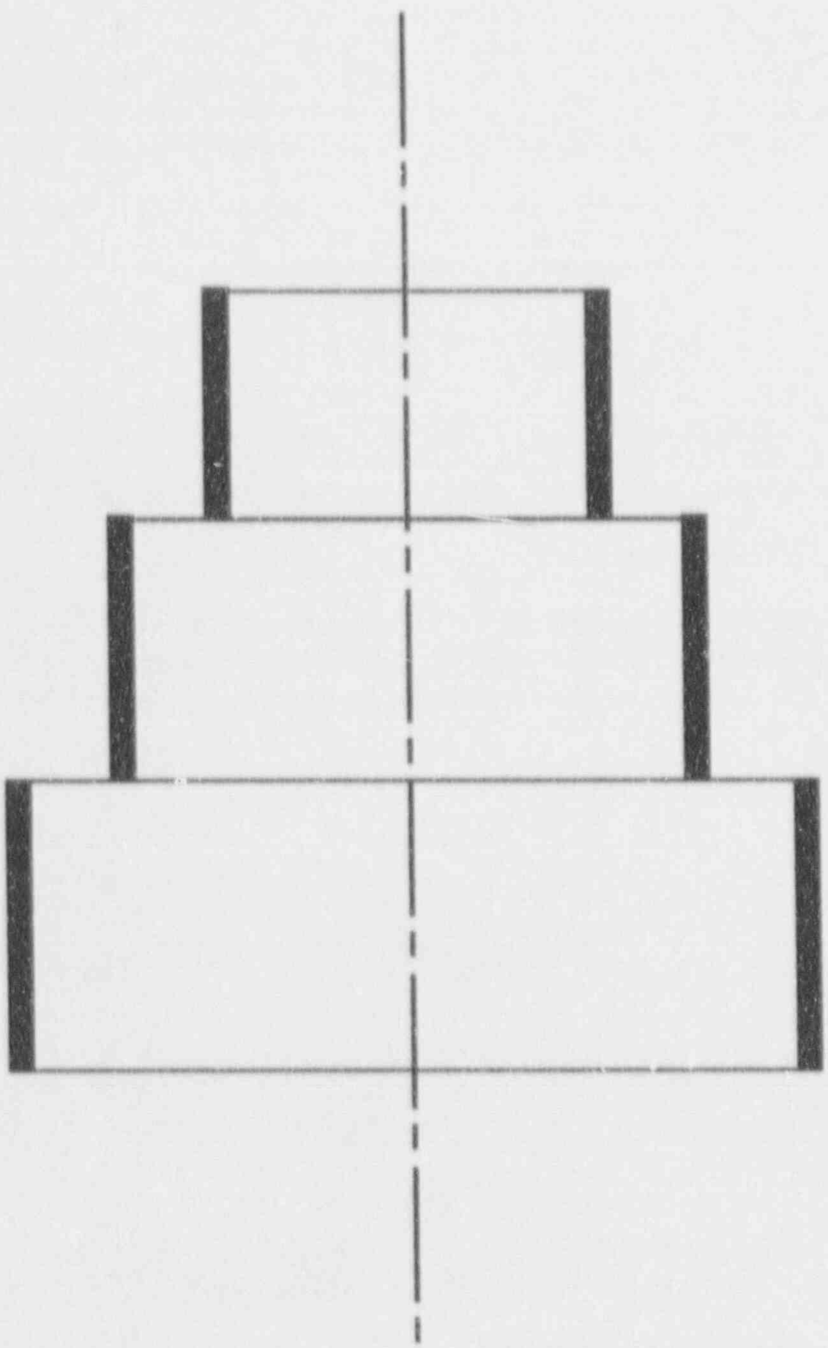

Figure 4-1 Radial displacement of basic lead slump model.

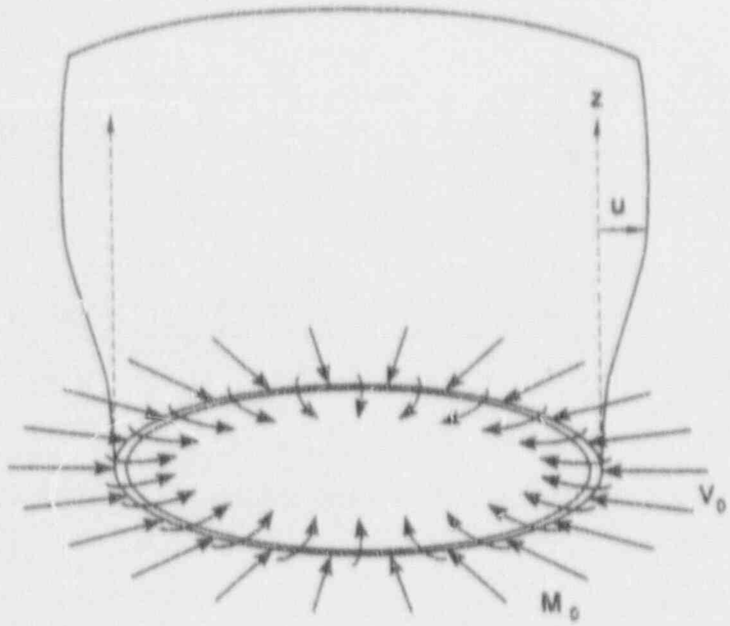

Figure 4-2 Bending and shear at the edge of a clamped cylindrical shell.

where

$$\lambda = \left[\frac{3(1-v^2)}{R^2 t^2} \right]^{0.25} ,$$

D = $Et^3/12(1-v^2)$,

E = Young's modulus,

v = Poisson's ratio,

R = radius of the shell,

t = thickness of the shell, and

x = axial distance from the end where the boundary condition is being considered.

If the edge of the cylinder is displaced radially without a rotation as shown in Fig. 4-2, the edge shear and moment must be related as follows:

$$V_o = 4D\lambda^3 u_o , \quad (4\text{–}28)$$

$$M_o = -2D\lambda^2 u_o , \quad (4\text{–}29)$$

where u_o is the radial displacement at the cylinder end. Equations 4-24 and 4-26 can be integrated over the element length ℓ to give the average radial displacement produced by the applied shear and moment in the element; i.e., for an end with an applied shear,

$$\bar{u} = \frac{u_o}{2\lambda\ell} [1 + e^{-\lambda\ell} (\sin\lambda\ell - \cos\lambda\ell)] , \quad (4\text{–}30)$$

where u_o is the radial displacement at the end.

For a fixed end, where the rotation vanishes and the shear is related to the moment according to Eqs. 4-28 and 4-29

$$\bar{u} = \frac{u_o}{\lambda\ell} e^{-\lambda\ell} \sin\lambda\ell . \quad (4\text{–}31)$$

These equations for average displacement are used to obtain the necessary displacement adjustment for simulating the effect of non-uniform radial displacement. For Case 1 of the two cases shown in Figure 4-3, where the element for which the displacement correction is obtained is identified as the ith element and is located between two adjoining elements, the (i-1) and (i+1)th elements, the displacement correction u_c to be added to the basic lead-slump solution is given as follows:

$$u_c = \frac{1}{4}(u_{i-1} + u_{i+1} - 2u_i)\left[\frac{1 + e^{-\lambda\ell}(\sin\lambda\ell - \cos\lambda\ell)}{\lambda\ell}\right] . \qquad (4\text{-}32)$$

where u_{i-1} , u_i , u_{i+1} are the radial displacement of the (i-1), i, and (i+1)th elements, respectively. These displacements are given by the basic lead-slump solution.

Similarly, for the other case (Case 2) in Fig. 4-3, where the (i-1)th element is replaced by a fixed boundary ($u = 0$ and $\psi = 0$), the displacement u_c can be obtained as follows:

$$u_c = \frac{1}{4}(u_{i+1} - u_i)\left[\frac{1 + e^{-\lambda\ell}(\sin\lambda\ell - \cos\lambda\ell)}{\lambda\ell}\right] - u_i\frac{e^{-\lambda\ell}\sin\lambda\ell}{\lambda\ell} . \qquad (4\text{-}33)$$

Using the corrected radial displacement of the element as u_0, the shear and moment at the fixed end of this element is obtained from Eqs. 4-28 and 4-29, respectively.

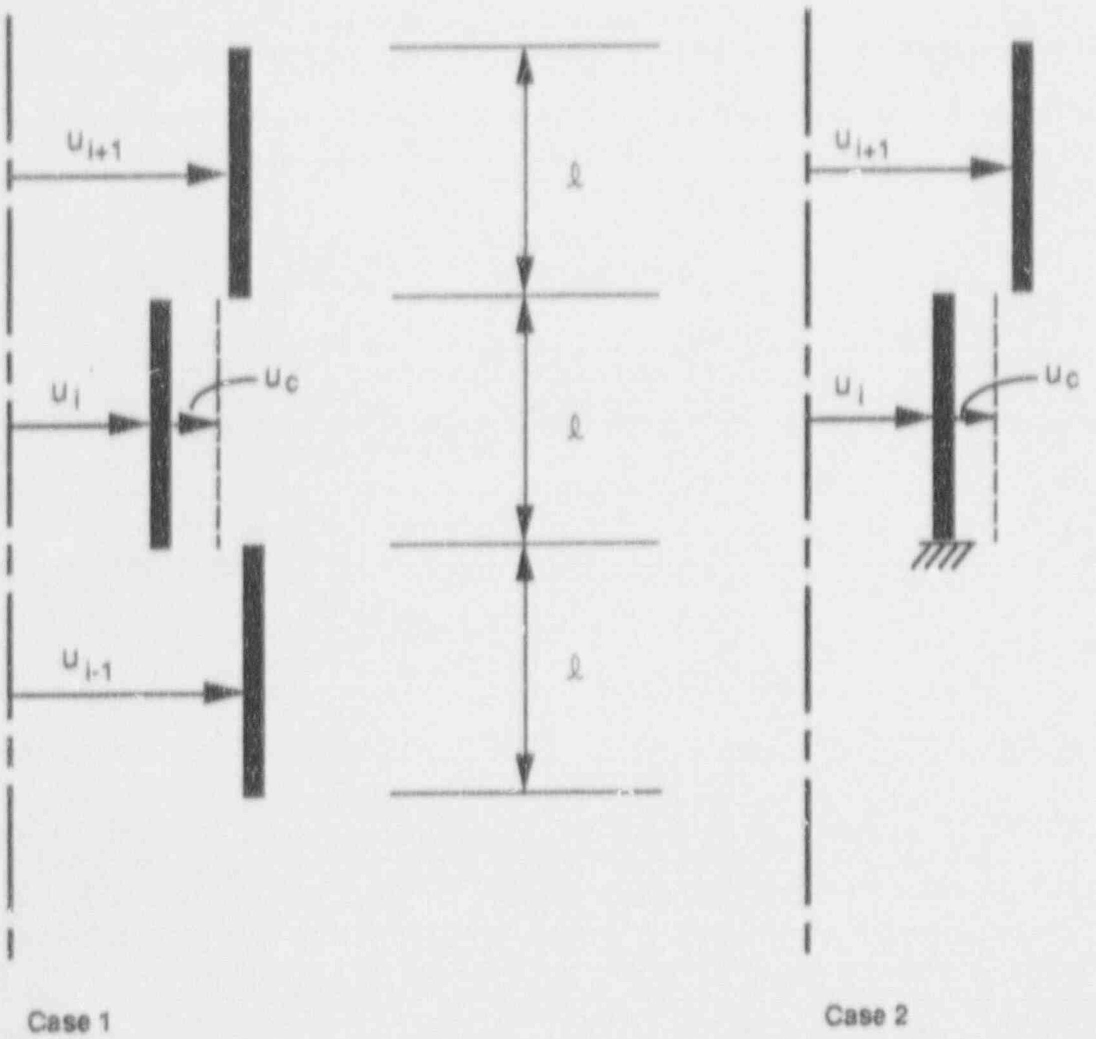

Figure 4-3 Displacement adjustment for simulating the effect of nonuniform radial displacement in the basic lead slump model.

5.0 PERMANENT LEAD SLUMP

The maximum permanent deformation produced by an impact in the lead shield of a shipping cask is important to the design of the cask because such a deformation can produce a sufficiently wide gap in the shield to damage the cask's capability for shielding radiation. In the present analysis, this change of the permanent deformation of the lead shield (LS: lead slump) can be calculated as the sum of the changes in permanent axial deformation of all lead elements of the analysis model; i.e.,

$$d\,LS = \sum_{i=1}^{n} (d\varepsilon_{zp}^{L})_i \, \ell_i \qquad (5\text{-}1)$$

where the subscript i is used to identify the quantities of the ith lead element ; ε_{zp}^{L} is the plastic axial strain of the lead element; and ℓ is the current element length.

The equation for calculating the change of plastic strain at each time step is given by the Prandtl-Reuss flow rule (Eq. 3-36); i.e.,

$$d\,\varepsilon_{zp}^{L} = \frac{3}{2}\,\frac{S_z^L}{\bar{\sigma}^L} \qquad (5\text{-}2)$$

Using Eq. 5-2, the permanent axial strain of a lead element can be determined after the stresses of the element are found (Step 8 in Section 4.3).

In SCANS, the lead slump is calculated and accumulated at each solution time step. The total lead slump is saved at specified time interval for plotting. Only the lead slump at the time of cask rebound is printed. The final lead slump can be smaller than the maximum value occurring during the impact because of possible reversed plastic flow produced by the high circumferential stress of the steel shells.

6.0 VERIFICATION OF IMPACT ANALYSIS CAPABILITIES OF SCANS

The SCANS computer program's quasi-static and dynamic analysis capabilities for impact study have been verified using hand calculations and the results of another computer program, NIKE (Ref. 15). Available analysis and test data found in the literature have also been used. The results of five sample problems used for the verification are summarized herein. Further details of the input and output of these problems are given in Appendix B of this report. Additional sample problems and results of the SCANS computer program can be found in Ref. 16.

The results reported herein are for 30-ft drops of three sample casks, namely the rail cask, the IF300 cask, and the Oak Ridge reduced-scale Hallam cask. Figure 6-1 depicts the geometry of a typical SCANS model for these casks. Figure 6-2 presents the force-deformation relations used for the impact limiters of these casks. The stiffness of the limiters varies over a wide range, from a rather soft one for Problems 1 and 2 to a nearly rigid one for Problem 4.

The basic verification of the SCANS program was carried out with the rail cask, for which SCANS results were compared to those of NIKE and of hand calculations. For the IF300 cask, SCANS' output for impact acceleration was compared with that published in Ref. 17. As for the Hallam cask, SCANS' prediction of the permanent slump of the unbonded lead shield was compared with Oak Ridge's test measurement (Ref. 18). As demonstrated in the following paragraphs, SCANS' results compare favorably with the others.

For the basic verification with the rail cask, hand-calculated results were obtained and compared for all printed output of SCANS' quasi-static analysis. The verified quasi-static results were then compared with those of SCANS' dynamic analysis. The hand calculations were facilitated using the Lotus 1-2-3 spreadsheet computer program. The formulas used for SCANS' quasi-static analysis were entered into a spreadsheet with appropriate input for impact conditions and cask geometry and materials. Results were obtained for drops with the cask's longitudinal axis oriented at various angles from horizontal. The cases analyzed included a drop at an angle of 0 degrees (a side drop), a drop at 90 degrees (an end drop), a drop at an angle where the cask's center of mass is located vertically above the impact point (a C.G. drop), and five other drops at 15, 30, 45, 60, and 75 degrees (oblique drops).

Tables 6-1 and 6-2 present the results of this analysis for the maximum limiter crush, impact acceleration, and force. All other results, such as stresses, are not presented herein but can be found in tabulated form in Appendix B. As seen in these tables, the "hand-calculated" results are almost identical to those from SCANS' quasi-static analysis. This close comparison of the two sets of results, however, is expected since the formulas used for both calculations are identical. The favorable comparison simply confirms that the formulas have been correctly implemented in SCANS. The compared results cover all the printed output of SCANS, namely, the maximum impact limiter crush; the maximum rigid body accelerations; the maximum impact forces and stress intensities in the cask shells and shield; and the maximum stresses in the end caps and the closure bolts.

In the tables just described, corresponding results from SCANS' dynamic analysis are also given. The dynamic analysis result for a given quantity in the tables represents the maximum value of the quantity that is reached during the primary, or the first, impact of the cask. The dynamic analysis of SCANS obtains results at each of all time steps, but only the maxima are equivalent and comparable to the quasi-static analysis results. The data presented in the tables show that the results of quasi-static and dynamic analyses are indeed comparable for all but a few cases. The exceptions are the oblique drops at an angle smaller than 45 degrees. For drops at a small angle, relatively larger differences are observable between the two sets of results. This situation is mainly due to some simplified assumptions used in SCANS' quasi-static analysis. For all oblique impacts, SCANS' quasi-static analysis assumes that only one of the two cask ends will be impacting the ground at a given time. Thus the impact force is always only applied at one end.

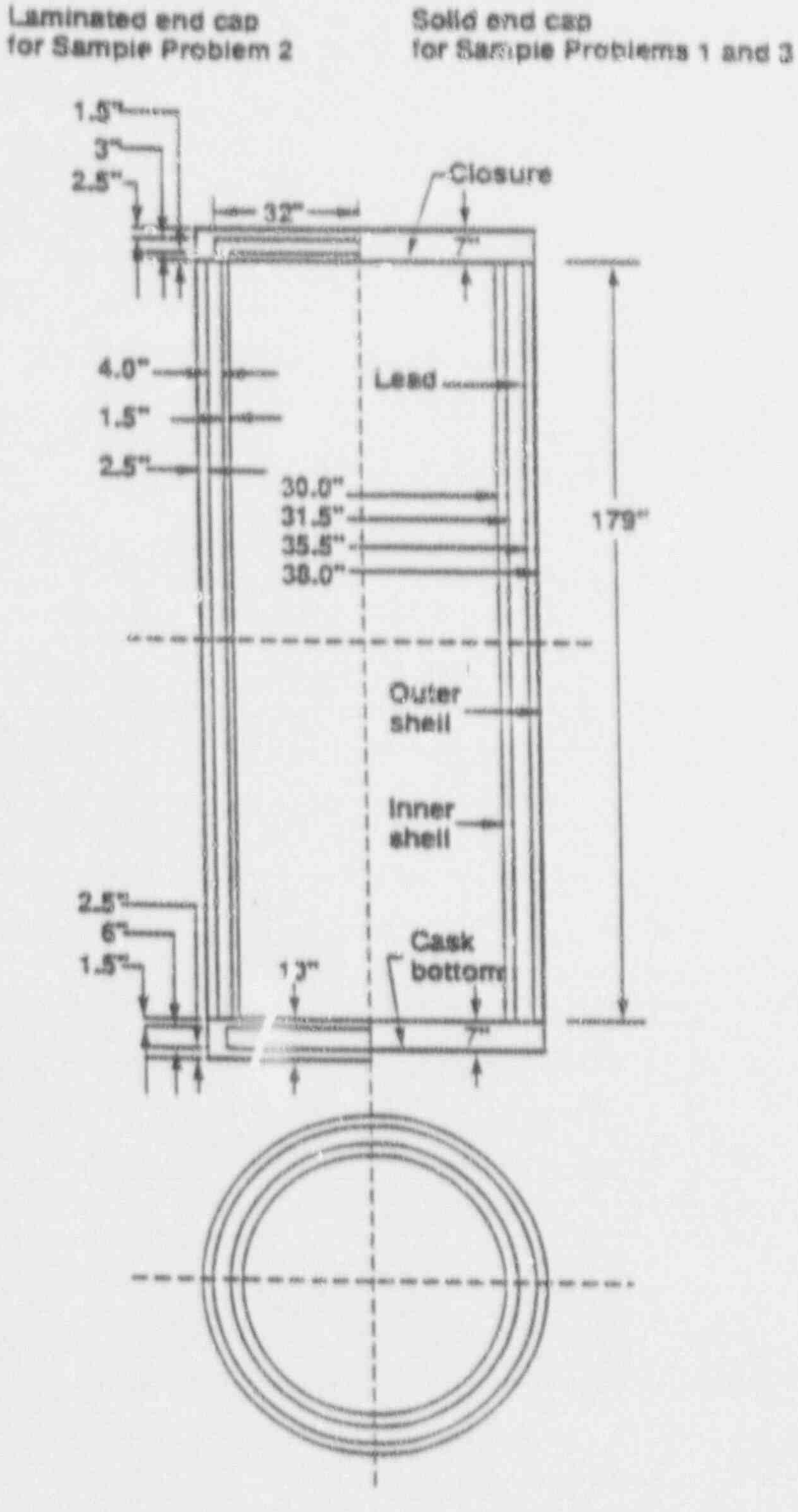

Figure 6-1 A typical SCANS model of shipping cask (dimensions are shown for the rail cask of Sample Problems 1, 2, and 3).

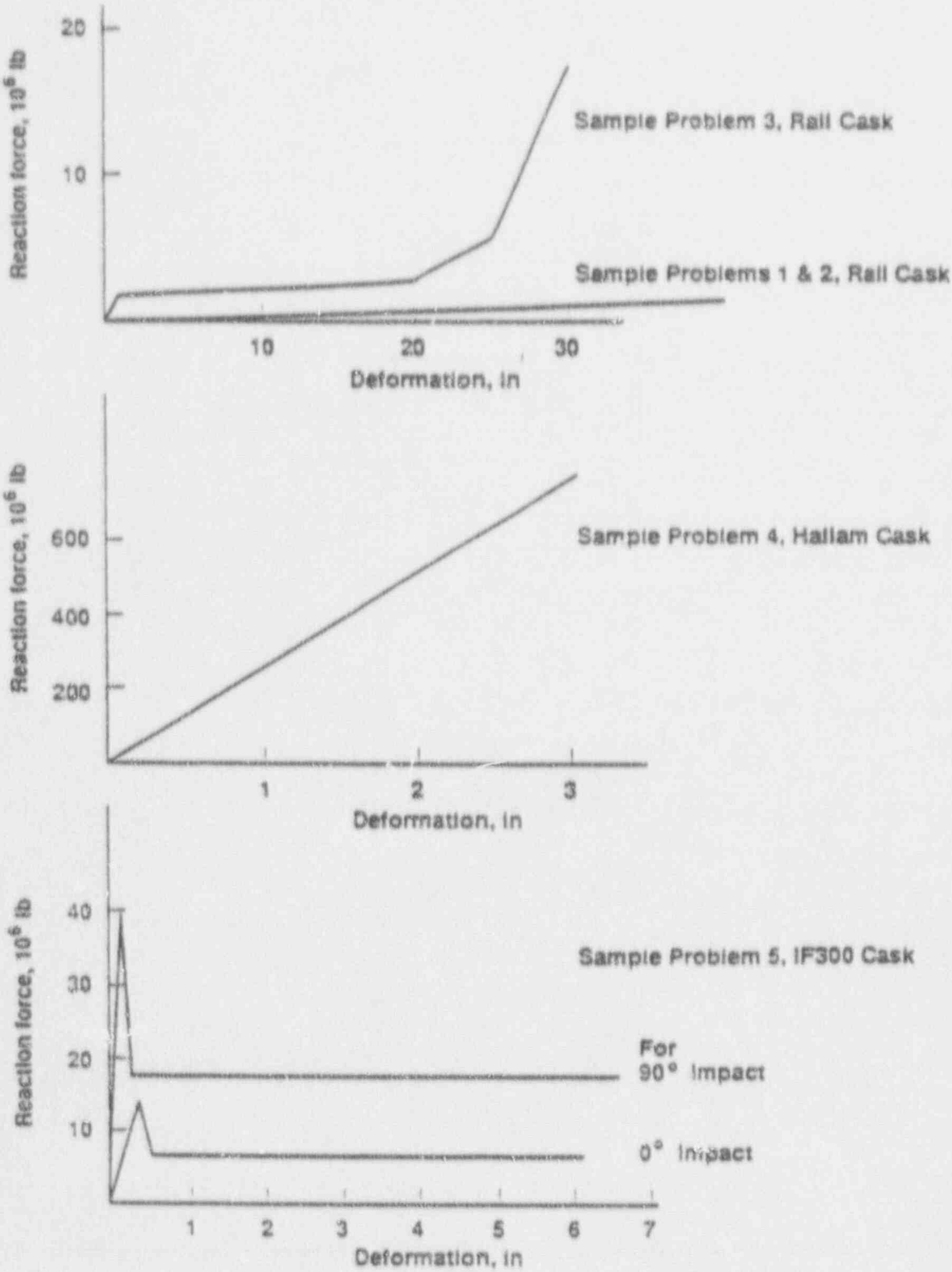

Figure 6-2 Force-deformation relations of impact limiter for verification problems.

Table 6-1 Comparison of SCANS results for maximum impact limiter crush and acceleration generated by impact at various angles (Sample Problem 1).

Primary Impact Angle (deg)	Max. Limiter Crush (in)			Max. Vertical Acceleration (g)			Max. Rot. Accel.(in/sec/sec)		
	Quasi-static		Dynamic	Quasi-static		Dynamic	Quasi-static		Dynamic
	Hand Calc	SCANS	SCANS	Hand Calc	SCANS	SCANS	Hand Calc	SCANS	SCANS
0.0	46.1	46.1	49.2	14.6	14.6	15.6	0.0	0.0	0.0
15.0	47.7	47.7	41.4	7.1	7.1	11.5	-62.2	-62.2	83.8
30.0	55.4	55.4	46.9	8.4	8.4	6.9	-55.9	-55.9	-58.2
45.0	61.4	61.4	56.0	9.4	9.4	8.5	-39.7	-39.7	-53.6
60.0	64.7	64.7	67.6	10.0	10.0	10.4	-15.5	-15.5	-35.2
75.0	64.9	64.9	68.9	10.0	10.0	10.7	11.9	11.9	29.6
90.0	65.2	65.2	71.4	10.0	10.0	11.1	0.0	0.0	0.0
[illegible]	65.2	65.2	71.4	10.0	10.0	11.1	-0.0	0.0	0.0

TABLE 6-2 Comparison of SCANS results for maximum impact force/moment generated by impact at various angles (Sample Problem 1).

Primary Impact Angle (deg)	Max. Axial Impact Force (kip)			Max. Impact Moment (in-kip)		
	Quasi-static		Dynamic	Quasi-static		Dynamic
	Hand Calc	SCANS	SCANS	Hand Calc	SCANS	SCANS
0.0	0.0	0.0	0.8	5379.7	5379.7	5750.9
15.0	-411.4	-411.4	-116.4	-4885.3	-4885.3	7907.5
30.0	-922.8	-922.8	-514.4	-23878.0	-23878.0	-14405.8
45.0	-1446.3	-1446.3	-1023.8	-44836.7	-44836.7	-32471.9
60.0	-1867.6	-1867.6	-1756.4	-63421.4	-63421.4	-58938.0
75.0	-2090.0	-2090.0	-2278.0	-75498.6	-75498.6	-84494.7
90.0	-2173.7	-2173.7	-2379.4	0.0	0.0	0.0
C.G.	-2022.6	-2022.6	-2214.0	-71282.1	-71282.1	-78043.1

While this assumption holds for oblique impacts at a large angle, it may not be realistic for impacts at a small angle, where both ends can be impacting at the same time. SCANS' dynamic analysis, on the other hand, does not make any assumption concerning impact ends; instead, it follows the development of an impact and describes the situation realistically. The dynamic analysis also evaluates, while the quasi-static analysis ignores, the centrifugal forces associated with a rotating cask. This difference in the treatment of the centrifugal force explains the relatively larger discrepancies seen between the quasi-static and dynamic results for the axial force in oblique impacts. Other than the foregoing differences between the dynamic and quasi-static analyses for oblique impacts, the results of the two analyses compare closely. This favorable comparison provides some assurance that the dynamic analysis of SCANS has also been properly implemented.

The favorable comparison of the quasi-static and the dynamic analysis results can be viewed as a mutual verification of these two capabilities of SCANS, since they are completely different in solution method and programming. However, the user of the program should be informed that other cases, in addition to the foregoing cases of small-angle oblique impacts, may show quite different results from SCANS' quasi-static and dynamic analyses. This difference is not due to incorrect implementation of the methods in SCANS, but to the basic limitation of the quasi-static analysis method. The quasi-static analysis of impact is based on the assumption that the cask behaves similarly to a rigid body during impact. The dynamic and the quasi-static analyses would agree only if this assumption holds, as in the cases where the impact duration is relatively long compared to the longest natural vibration period of the cask. Casks with relatively soft limiters usually meet this condition. Sample Problems 1–3 are such cases and their results can, therefore, be used for the mutual verification of the two analysis options of SCANS. For casks with very stiff limiters, Ref. 6 has already shown that SCANS' quasi-static and dynamic analyses can indeed produce very different results. As a general rule, the quasi-static analysis should not be used for casks with stiff limiters and for oblique drops at small angles.

An end drop of the rail cask (Sample Problem 3) has also been analyzed with the NIKE computer program. The results are compared to SCANS' in Tables 6-3-1 and 6-4-2. The comparison is made for casks with bonded and unbonded lead shields in the maximum limiter crush, the maximum rigid-body acceleration, and the maximum stresses. The results for the unbonded shield provide a detailed verification of SCANS' lead-slump-analysis method as presented in this report. For both the bonded and unbonded shields, the comparison of NIKE's and SCANS' results is reasonably good, considering the vast difference between the two computer programs and models. The NIKE program is a well-known, sophisticated, finite element, mainframe computer program for general impact studies. It uses solid finite elements, compared to the beam element of SCANS.

As shown in Fig. 6-3, the NIKE computer model for the foregoing analysis is made of axisymmetric solid elements. For each of the shells and shield of the cask, 2 and 50 layers of the elements are used in the radial and longitudinal directions, respectively. The solid elements are also used to model the impact limiters. Elastic and plastic properties of the impact limiters are adjusted to match the force-deformation relation of the impact limiters given in Fig. 6-2 for SCANS model of Sample Problem 3. The NIKE stress results listed in Table 6-3-2 are average values over the radial thickness of the shells and shield. The stress is not uniform across the thickness, especially in cross sections near the two cask ends, where the end effect described in Section 4.4 of this report is expected to be prominent. In agreement with this expectation, a bending effect is evident in the distribution of the NIKE stress results. However, this bending effect is not included in all the stress results presented.

Comparing the results presented in Tables 6-3-1 and 6-3-2 for bonded and unbonded shields, the effect of unbonded lead shield on the shell stresses can be easily recognized. As expected, without the support of the steel shells in the axial direction, the unbonded lead shield shows much higher axial stress and deformation than a bonded one. Because of the Poisson's effect in the shield material, this higher axial deformation of the unbonded shield causes higher radial deformations in

Table 6-3-1 Comparison of results for casks with bonded and unbonded lead shield obtained using the NIKE and SCANS computer programs (Sample Problem 3, 90-degree impact).

Shield Type	Elastic Properties of Lead Shield: Young's Modulus (psi)	Poisson's Ratio	Analysis Method	Maximum Limiter Crush (in)	Maximum Vertical Accel (g)	Maximum Principal Stresses (psi) Axial Location 22" from Impact End: Inner Shell	Lead Shield	Outer Shell
Bonded	25000	0.43	SCANS (Quasi-static)	25.9	38.2	5045	4	5045
			SCANS (Dynamic)	26.5	45.6	6644	6	6644
			NIKE (Dynamic)	26.0	43.0	7532	7	5225
Unbonded	25000	0.43	SCANS (Quasi-static)	25.9	38.2	30739	1051	21204
			SCANS (Dynamic)	26.5	45.6	33009	1127	24069
			NIKE (Dynamic)	25.9	40.3	25435	1066	19400
Bonded	2220000	0.43	SCANS (Quasi-static)	25.9	38.2	4692	368	4692
			SCANS (Dynamic)	26.5	45.5	6438	505	6438
			NIKE (Dynamic)	26.3	42.0	7358	452	5590
Unbonded	2220000	0.43	SCANS (Quasi-static)	25.9	38.2	3008	2457	4177
			SCANS (Dynamic)	26.5	45.5	4114	3176	5734
			NIKE (Dynamic)	26.3	41.8	4157	3049	4721

Note: The lead property values used to obtain the results in this table are for parametric study only. The current SCANS program uses a different set of values for the properties and, therefore, will not reproduce SCANS results shown herein.

Table 6-3-2 Comparison of results for casks with bonded and unbonded lead shield as obtained using the NIKE and SCANS computer programs (Sample Problem [illegible], 90-degree impact).

Elastic Properties of Lead Shield				[illegible] at Axi[illegible] [illegible]ation 22" from Impact End								
				Inner Ste[illegible]			Lead Shield			Outer Steel Shell		
Shield Type	Young's Modulus (psi)	Poisson's Ratio	Analysis Method	Axial Stress	Radial Stress	[illegible]	[illegible]	Radial Stress	Circ Stress	Axial Stress	Radial Stress	Circ Stress
Bonded	25000	0.43	SCANS (Quasi-static)	-5045	0	0	-4	0	0	-5045	0	0
			SCANS (Dynamic)	-6644	0	0	-6	0	0	-6644	0	0
			NIKE (Dynamic)	-7550	-18	-440	-18	-12	-11	-5050	-17	175
Unbonded	25000	0.43	SCANS (Quasi-static	-12634	0	-30739	-2530	-1479	-1725	0	0	21204
			SCANS (Dynamic)	-12834	0	-33009	-2713	-1586	-1807	-1373	0	22696
			NIKE (Dynamic)	-7540	-615	-26049	-2255	-1189	-1487	-1385	-566	18015
Bonded	2220000	0.43	SCANS (Quasi-static)	-4692	0	0	-368	0	0	-4692	0	0
			SCANS (Dynamic)	-6438	0	0	-505	0	0	-6438	0	0
			NIKE (Dynamic)	-6193	5	1166	-467	-22	-15	-4715	-36	875
Unbonded	2220000	0.43	SCANS (Quasi-static)	-3008	0	-265	-2530	-73	-993	-2403	0	1774
			SCANS (Dynamic)	-4114	0	-395	-3267	-91	-1231	-3529	0	2205
			NIKE (Dynamic)	-4181	-24	-604	-3152	-103	-1262	-2362	85	2359

Note: The lead property values used to obtain the results in this table are for parametric study only. The current SCANS program uses a different set of values for the properties and, therefore, will not reproduce the SCANS results shown herein.

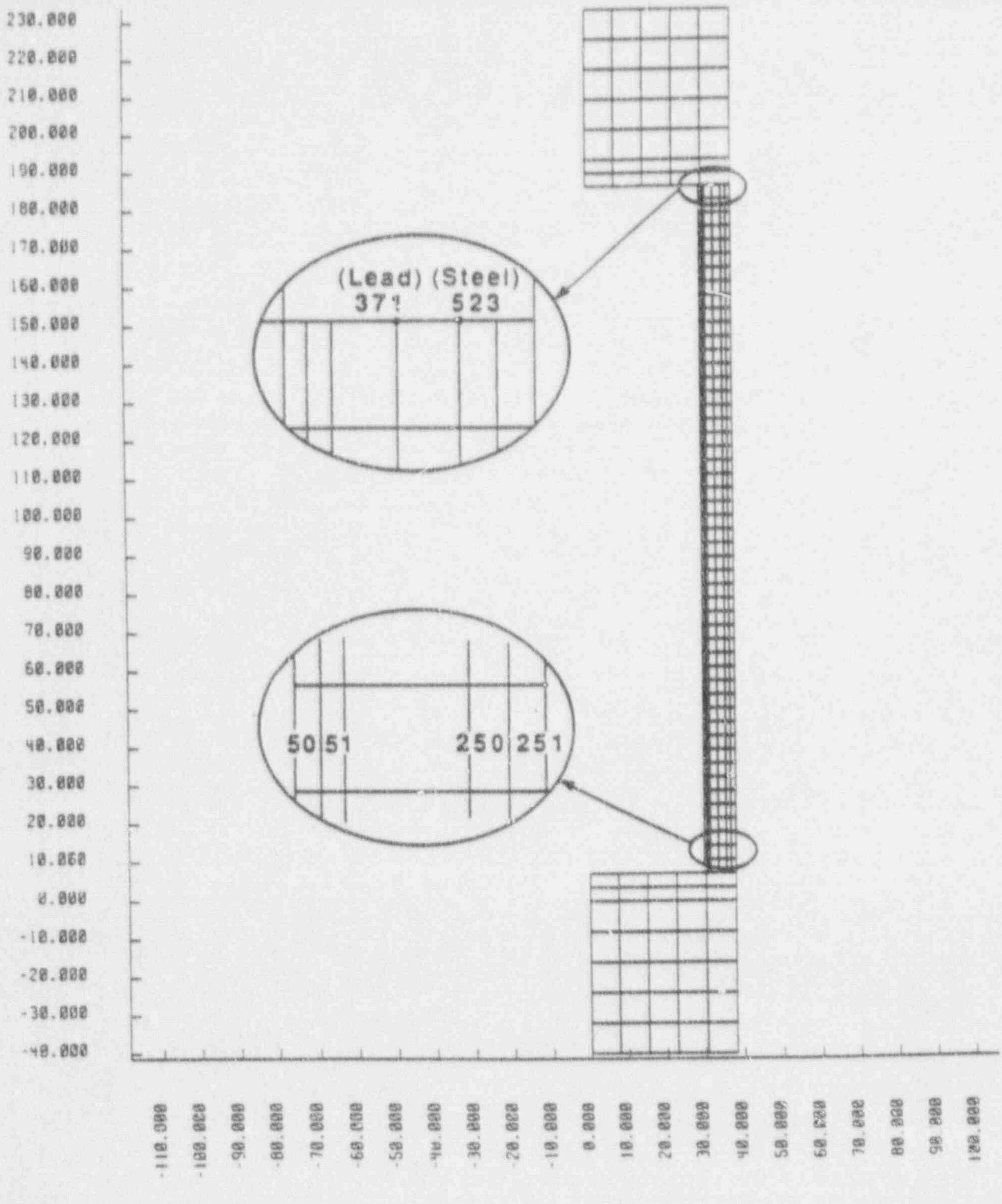

Figure 6-3 NIKE2D finite element model of a rail cask including impact limiters (dimensions are in inches).

the inner and outer steel shells as well as in the shield. These higher radial deformations in turn cause more prominent hoop stresses to develop in the shells. Finally, through the Poisson's effect of the shell material, the axial stresses in the shells are also affected. The results in Table 6-3-1 and 6-3-2 are elastic solutions obtained using two greatly different values for the Young's modulus of the lead shield. Despite the large change in modulus value, the SCANS program is able to give results comparable to NIKE's for both cases. Thus one can conclude that the SCANS model developed in this report is adequate for the analysis of the lead slump effect on the stresses in the cask. This conclusion is valid even when the lead deforms plastically, as shown in the following results of a study using the NIKE computer program.

Tables 6-4-1 and 6-4-2 present the results of this study, which were obtained for lead shields having a bi-linear stress-strain relation defined by the yield stress and the Young's and plastic moduli given in the tables. Results for lead slump, and stresses of the lead and steel shells at two axial locations (22" and 44"), are given in the table for eight cases. These cases have greatly different yield stresses and moduli. The yield stress varies from 250 to 4300 psi, the Young's modulus from 2500 to 2,220,000 psi, and the plastic modulus from 500 to 25,000 psi. Despite these wide variations in lead properties, SCANS appears capable of producing results comparable to NIKE's. Both sets of results show the same general trends of change when the lead properties vary; i.e., the magnitude of the lead slump, the radial stress of the lead shield, and the hoop stress of the steel shells increase rapidly with decreasing moduli and yield stress of the lead shield. The agreement between SCANS and NIKE results, however, appears to be closer for cases with purely elastic than with elastic-plastic deformation. This better performance for elastic case is expected because the elastic-plastic deformation is difficult for SCANS' simplified model to describe accurately. In general, the comparison of SCANS and NIKE results in Tables 6-4-1 and 6-4-2 shows that the present SCANS lead-slump model provides reasonable results for confirmatory evaluation of the lead-slump effect on shipping casks. Table 6-5 provides additional evidence for this claim. The results presented in this table shows that the SCANS prediction for the lead slump of the Hallam cask (Sample Problem 4) compares closely with the Oak Ridge test result.

Table 6-4-1 Effect of Elastic, Plastic Properties of Lead on Maximum Lead Slump and Principal Stresses for Cask with Unbonded Lead Shield (Comparison of SCANS and NIKE results for Sample Problem 3, 90-degree Impact) - Continued

Case ID	Elastic Properties of Lead Shield: Young's Modulus (psi)	Elastic Properties of Lead Shield: Poisson's Ratio	Plastic Properties of Lead Shield: Plastic Modulus (psi)	Plastic Properties of Lead Shield: Yield Stress (psi)	Solution	Maximum Limiter Crush (in)	Maximum Vertical Accel (g)	Permanent Axial Deform. Of Lead Shield (in)	Axial Location: Distance from Impact End (in)	Maximum Principal Stresses At Axial Location (psi): Inner Shell	Lead Shield	Outer Shell
H	[illegible]20000	0.43	25000	4300	SCANS (Q-static)	25.9	38.2	0.00	22	3008	2457	4177
					SCANS (Dynamic)	26.5	45.5	0.00		4114	3176	5734
					NIKE (Dynamic)	26.3	41.8	0.00		4157	3049	4721
					SCANS (Q-static)				44	2732	2106	3706
					SCANS (Dynamic)					3783	2738	5264
					NIKE (Dynamic)					3937	2794	4135
J	2220000	0.43	25000	1250	SCANS (Q-static)	25.9	38.2	0.42	22	16077	1778	13692
					SCANS (Dynamic)	26.5	45.5	0.37		14775	2960	15086
					NIKE (Dynamic)	26.2	41.5	0.54		22185	1741	18323
					SCANS (Q-static)				44	10412	1621	9852
					SCANS (Dynamic)					10664	2805	11988
					NIKE (Dynamic)					15978	1614	13767
I	2220000	0.43	25000	750	SCANS (Q-static)	25.9	38.2	0.42	22	25681	1267	19268
					SCANS (Dynamic)	26.5	45.5	0.37		17276	2390	15079
					NIKE (Dynamic)	26.1	40.0	1.22		27756	1483	22789
					SCANS (Q-static)				44	20047	1177	15417
					SCANS (Dynamic)					12514	2307	11845
					NIKE (Dynamic)					25405	1242	23455

Table 6-4-1 Continued

Case ID	Elastic Properties of Lead Shield: Young's Modulus (psi)	Elastic Properties of Lead Shield: Poisson's Ratio	Plastic Properties of Lead Shield: Plastic Modulus (psi)	Plastic Properties of Lead Shield: Yield Stress (psi)	Solution	Maximum Limiter Crush (in)	Maximum Vertical Accel (g)	Permanent Axial Deform. Of Lead Shield (in)	Axial Location: Distance from Impact End (in)	Maximum Principal Stresses At Axial Location (psi): Inner Shell	Maximum Principal Stresses At Axial Location (psi): Lead Shield	Maximum Principal Stresses At Axial Location (psi): Outer Shell
K	2220000	0.43	25000	500	SCANS (Q-static)	25.9	38.2	1.16	22	30493	1045	22061
					SCANS (Dynamic)	26.5	45.5	1.47		28934	2002	22583
					NIKE (Dynamic)	26.1	39.9	1.41		28314	1378	23227
					SCANS (Q-static)				44	31716	639	23836
					SCANS (Dynamic)					31712	1557	23845
					NIKE (Dynamic)					28059	1129	21287
E	2220000	0.43	25000	250	SCANS (Q-static)	25.9	38.2	1.49	22	35308	822	24857
					SCANS (Dynamic)	26.5	45.5	1.91		32563	1837	24903
					NIKE (Dynamic)	26.1	39.7	1.27		28498	1313	22762
					SCANS (Q-static)				44	38866	308	26832
					SCANS (Dynamic)					36659	1445	27214
					NIKE (Dynamic)					28109	939	21464
M	2220000	0.43	2500	500	SCANS (Q-static)	25.9	38.2	1.50	22	38764	663	27321
					SCANS (Dynamic)	26.5	45.5	1.61		31110	1893	23821
					NIKE (Dynamic)	26.0	40.4	1.37		28921	765	23734
					SCANS (Q-static)				44	26346	901	18174
					SCANS (Dynamic)					34525	1546	25654
					NIKE (Dynamic)					27950	648	20589

Table 6-4-1 Concluded

Case ID	Elastic Properties of Lead Shield: Young's Modulus (psi)	Elastic Properties of Lead Shield: Poisson's Ratio	Plastic Properties of Lead Shield: Plastic Modulus (psi)	Plastic Properties of Lead Shield: Yield Stress (psi)	Solution	Maximum Limiter Crush (in)	Maximum Vertical Accel (g)	Permanent Axial Deform. Of Lead Shield (in)	Axial Location: Distance from Impact End (in)	Maximum Principal Stresses At Axial Location (psi): Inner Shell	Lead Shield	Outer Shell
L	2220000	0.43	500	250	SCANS (Q-static)	25.9	38.2	1.93	22	45963	331	31637
					SCANS (Dynamic)	26.5	45.5	2.07		35303	1604	26555
					NIKE (Dynamic)	26.0	42.0	1.94		29897	348	23762
					SCANS (Q-static)				44	38866	308	26832
					SCANS (Dynamic)					39548	1152	28949
					NIKE (Dynamic)					28419	267	19865
C	25000	0.43	500	2500	SCANS (Q-static)	25.9	38.2	0.00	22	30739	1051	21204
					SCANS (Dynamic)	26.5	45.6	0.00		33009	1127	24069
					NIKE (Dynamic)	25.9	40.3	0.00		25435	1066	19400
					SCANS (Q-static)				44	26346	901	18174
					SCANS (Dynamic)					30026	1032	22013
					NIKE (Dynami_)					22184	965	16984

Table 6-4-2 Effect of Elastic, Plastic Properties of Lead on Maximum Lead-Slump Stresses for Cask with Unbonded Lead Shield (Comparison of SCANS and NIKE results for Sample Problem 3, 90-degree Impact) - Continued

Case ID	Elastic Properties of Lead Shield: Young's Modulus (psi)	Elastic Properties of Lead Shield: Poisson's Ratio	Plastic Properties of Lead Shield: Plastic Modulus (psi)	Plastic Properties of Lead Shield: Yield Stress (psi)	Solution	Axial Location: Distance from Impact End (in)	Inner Steel Shell: Axial Stress	Inner Steel Shell: Radial Stress	Inner Steel Shell: Circ Stress	Lead Shield: Axial Stress	Lead Shield: Radial Stress	Lead Shield: Circ Stress	Outer Steel Shell: Axial Stress Min.	Outer Steel Shell: Axial Stress Max.	Outer Steel Shell: Radial Stress	Outer Steel Shell: Circ Stress
N	2220000	0.43	25000	4300	SCANS (Q-static)	22	-3008	0	-265	-2530	-73	-993	-2403	0	0	1774
					SCANS (Dynamic)		-4114	0	-395	-3267	-91	-1231	-3529	15	0	2205
					NIKE (Dynamic)		-4181	-24	-604	-3152	-103	-1260	-2362	619	-85	2359
					SCANS (Q-static)	44	-2732	0	-263	-2169	-63	-848	-2191	0	0	1515
					SCANS (Dynamic)		-3783	0	-360	-2821	-83	-1115	-3266	67	0	1998
					NIKE (Dynamic)		-3950	-14	-634	-2883	-89	-1166	-2139	639	-70	1996
J	2220000	0.43	25000	1250	SCANS (Q-static)	22	-8055	0	-16077	-2530	-753	-1680	-1358	0	0	12334
					SCANS (Dynamic)		-8099	0	-14775	-3753	-793	-2202	-2699	1982	0	12387
					NIKE (Dynamic)		-6036	-528	-22713	-2811	-1070	-1906	-1659	1422	-529	16664
					SCANS (Q-static)	44	-5998	0	-10412	-2169	-548	-1355	-1440	0	0	8412
					SCANS (Dynamic)		-6658	0	-10664	-3393	-588	-1848	-2639	1372	0	9349
					NIKE (Dynamic)		-5806	-398	-16376	-2460	-847	-1603	-1456	1426	-425	12311
I	2220000	0.43	25000	750	SCANS (Q-static)	22	-11067	0	-25681	-2530	-1264	-1902	-818	1731	0	18450
					SCANS (Dynamic)		-8858	0	-17276	-3286	-896	-2057	-1423	2571	0	13656
					NIKE (Dynamic)		-10194	-902	-28657	-2830	-1347	-2146	-1151	2754	-511	21638
					SCANS (Q-static)	44	-9041	0	-20047	-2169	-992	-1578	-865	993	0	14552
					SCANS (Dynamic)		-6990	0	-12514	-2971	-664	-1735	-1562	1817	0	10283
					NIKE (Dynamic)		-8026	-638	-26043	-2503	-1261	-1851	-1027	2744	-628	22429

Table 6-4-2 Continued

Case ID	Elastic Properties of Lead Shield: Young's Modulus (psi)	Elastic Properties of Lead Shield: Poisson's Ratio	Plastic Properties of Lead Shield: Plastic Modulus (psi)	Plastic Properties of Lead Shield: Yield Stress (psi)	Solution	Axial Location: Distance from Impact End (in)	Stresses (psi) At Axial Location: Inner Steel Shell: Axial Stress	Inner Steel Shell: Radial Stress	Inner Steel Shell: Circ Stress	Lead Shield: Axial Stress	Lead Shield: Radial Stress	Lead Shield: Circ Stress	Outer Steel Shell: Axial Stress Min.	Outer Steel Shell: Axial Stress Max.	Outer Steel Shell: Radial Stress	Outer Steel Shell: Circ Stress
K	2220000	0.43	25000	500	SCANS (Q-static)	22	-12573	0	-30493	-2530	-1486	-2012	-547	2510	0	21515
					SCANS (Dynamic)		-11911	0	-28934	-3442	-1440	-2432	-1351	5132	0	21232
					NIKE (Dynamic)		-9335	-807	-29122	-2768	-1390	-2124	-1005	3047	-644	22222
					SCANS (Q-static)	44	-10551	0	-24832	-2169	-1213	-1689	-579	1755	0	17601
					SCANS (Dynamic)		-12155	0	-31712	-3115	-1558	-2321	-1113	5546	0	22732
					NIKE (Dynamic)		-9151	-738	-28797	-2548	-1419	-2021	-856	2927	-699	20431
E	2220000	0.43	25000	250	SCANS (Q-static)	22	-14073	0	-35308	-2530	-1708	-2123	-276	3295	0	24581
					SCANS (Dynamic)		-12816	0	-32563	-3447	-1610	-2547	-1290	5549	0	23613
					NIKE (Dynamic)		-9769	-823	-29321	-2704	-1391	-2103	-821	3892	-683	219[illegible]
					SCANS (Q-static)	44	-12056	0	-29603	-2169	-1433	-1799	-292	2515	0	20640
					SCANS (Dynamic)		-13651	0	-36659	-3235	-1790	-2480	-1256	6166	0	25959
					NIKE (Dynamic)		-9665	-735	-28844	-2357	-1418	-1927	-769	3526	-700	20694
M	2220000	0.43	2500	500	SCANS (Q-static)	22	-15199	0	-38764	-2530	-1867	-2201	-542	3809	0	26779
					SCANS (Dynamic)		-12381	0	-31110	-3435	-1542	-2500	-1161	5549	0	22661
					NIKE (Dynamic)		-9955	-899	-29820	-2256	-1490	-1906	-984	4965	-723	22750
					SCANS (Q-static)	44	-12728	0	-31716	-2169	-1530	-1849	-576	2846	0	21987
					SCANS (Dynamic)		-12861	0	-34525	-3235	-1689	-2420	-1114	6041	0	24540
					NIKE (Dynamic)		-10142	-764	-28714	-2077	-1428	-1775	-944	4726	-697	19645

Table 6-4-2 Concluded

Case ID	Elastic Properties of Lead Shield: Young's Modulus (psi)	Elastic Properties of Lead Shield: Poisson's Ratio	Plastic Properties of Lead Shield: Plastic Modulus (psi)	Plastic Properties of Lead Shield: Yield Stress (psi)	Solution	Axial Location: Distance from Impact End (in)	Stresses (psi) At Axial Location — Inner Steel Shell: Axial Stress	Inner Steel Shell: Radial Stress	Inner Steel Shell: Circ Stress	Lead Shield: Axial Stress	Lead Shield: Radial Stress	Lead Shield: Circ Stress	Outer Steel Shell: Axial Stress Min.	Outer Steel Shell: Axial Stress Max.	Outer Steel Shell: Radial Stress	Outer Steel Shell: Circ Stress
L	2220000	0.43	500	250	SCANS (Q-static)	22	-17471	0	-45963	-2530	-2199	-2366	-274	4954	0	31363
					SCANS (Dynamic)		-13720	0	-35303	-3337	-1733	-2549	-1301	6247	0	25254
					NIKE (Dynamic)		-11057	-1066	-30963	-1890	-1542	-1736	-775	5895	-725	22987
					SCANS (Q-static)	44	-14988	0	-38866	-2169	-1861	-2014	-291	3981	0	26542
					SCANS (Dynamic)		-14429	0	-39548	-3071	-1919	-2483	-1261	6873	0	27688
					NIKE (Dynamic)		-11057	-777	-29196	-1647	-1379	-1507	-698	5830	-691	19167
C	25000	0.43	500	2500	SCANS (Q-static)	22	-12634	0	-30739	-2530	-1479	-1725	0	2430	0	21204
					SCANS (Dynamic)		-12834	0	-33009	-2713	-1586	-1807	-1373	6900	0	22696
					NIKE (Dynamic)		-7540	-615	-26049	-2255	-1189	-1487	-1385	3006	-566	18015
					SCANS (Q-static)	44	-10959	0	-26346	-2169	-1268	-1479	0	1952	0	18174
					SCANS (Dynamic)		-10820	0	-30026	-2476	-1444	-1669	-1328	6369	0	20685
					NIKE (Dynamic)		-7274	-559	-22743	-2076	-1111	-1371	-1087	2942	-524	15896

Table 6-5 Comparison of results for permanent lead slump in unbonded lead shield generated by 30-ft end drop (Sample Problem 4).

Method of Prediction	Total Permanent Lead Shield Slump (in)
SCANS Dynamic Analysis	0.54
Oak Ridge Test (Ref. 18)	0.7
Design Guide Formula (Ref. 18)	0.62

The maximum limiter crush and acceleration results for the IF300 cask are given in Table 6-6. These results show that SCANS' quasi-static and dynamic analyses predict similar maximum values for these quantities. The similarity of results from the two SCANS analyses is also apparent in the results for the dynamic amplification factor, which show that the ratio of the dynamic to the quasi-static results for the maximum force/moment in the cask is near 1.0. The maximum value used for the calculation of the amplification factor given in Table 6-6 is the absolute maximum force/moment generated in the cask by the impact. For the 0-degree impact, the maximum moment at the center of the cask length is used. For the 90-degree impact, the maximum force at the impact end of the cask is used. For both impacts, the amplification factor has a value close to 1.0, indicating nearly equal quasi-static and dynamic solutions for the maximum force/moment of these cases. For comparison, the results given in Ref. 17 for the dynamic amplification factor and for the maximum acceleration are also listed in Table 6-6. The results compare closely with that of SCANS with only one exception: Ref. 17 gives a relatively more conservative estimate of the amplification factor for the 90-degree impact. This disagreement is probably due to the difference in analysis method and model. Reference 17 describes the reaction of the impact limiter using an assumed applied force time history, whereas the SCANS program models the impact limiter with a force-deformation relation. The effect of this difference in modeling is further amplified by the flexibility of the IF300 cask. SCANS dynamic analysis results indicate that for the impacts studied herein, the IF300 cask behaves more like a flexible body than a rigid body. Consequently, the discrepancies between the results of Ref. 17 and SCANS are reasonable.

In summary, this chapter has presented evidence to demonstrate the reliability of the quasi-static and dynamic analysis methods of SCANS computer program. The analysis methods produce results that are not only consistent with each other, but are also comparable with other independent analyses and tests. This chapter has also pointed out some possible limitations of the quasi-static analysis method; its results should be carefully reviewed and confirmed with the dynamic analysis for casks with stiff impact limiters and for drops at a small angle. By presenting the results of a study using the NIKE computer program, this chapter has also provided some insight into the reason for the observed success of SCANS' method for lead slump analysis.

Table 6-6 Comparison of impact analysis results for IF300 cask (Sample Problem 5).

Impact Angle (deg.)	Maximum Limiter Deform. (in)		Maximum Impact Force (kip)		Maximum Impact Acceleration (g)			Dynamic Amp. Factor	
	SCANS Q-static	SCANS Dynamic	SCANS Q-static	SCANS Dynamic	SCANS Q-static	SCANS Dynamic	Ref. 17	SCANS	Ref. 17
0.0	3.6	3.5	14310	14114	216.1	213.7	214.0	1.08	1.00
90.0	2.6	2.6	40140	39899	303.5	301.7	280.0	1.02	2.00

Notes:

1. SCANS' value for the dynamic amplification factor is the ratio of the dynamic analysis result to the quasi-static analysis result for the maximum force/moment in the cask body.

2. This sample problem uses depleted uranium for radiation shield. A material file for depleted uranium must be first created before running this sample problem.

REFERENCES

1. R. C. Chun, D. J. Trummer, and T. A. Nelson, "SCANS - Shipping Cask Analysis System, Vol. 2 Theory Manual, Impact Analysis," Lawrence Livermore National Laboratory, UCID-20674/Vol. 2; prepared for the U.S. Nuclear Regulatory Commission, NUREG/CR-4554 (1987).

2. T. A. Nelson and R. C. Chun, "Methods for Impact Analysis of Shipping Containers," Lawrence Livermore National Laboratory, UCID-20639; prepared for the U.S. Nuclear Regulatory Commission, NUREG/CR-3966 (1987).

3. J. S. Przemieniecki, Theory of Matrix Structural Analysis, McGraw-Hill Book Co. (1968).

4. R. Hill, "The Mathematical Theory of Plasticity," Oxford Univ. Press, New York (1950).

5. D. C. Drucker, "Plasticity and Viscoelasticity - Basic Concepts," Handbook of Engineering Mechanics, Chapter 46, W. Flugge, editor, McGraw Hill, New York (1962).

6. T. E. Tietz, "Mechanical Properties of a High Purity Lead and a 0.058 Percent Copper-Lead Alloy at Elevated Temperatures," *Proc. ASTM*, Vol. 59, p. 1052 (1959).

7. U. S. Lindholm, "Some Experiments with the Split Hopkinson Pressure Bar," *Journal of the Mechanics and Physics of Solids*, Vol. 12, 1964, p. 317 (1964).

8. C. H. Mok and J. Duffy, "The Dynamic-Stress Strain Relation of Metals as Determined from Impact Tests with a Hard Ball," *Int. J. of Mech. Sci.*, Vol. 7, p. 355 (1965).

9. S. J. Green, et al., "The High Strain-Rate Behavior of Face-Centered Cubic Metals," *Proceedings of the Battelle Colloquium Inelastic Behavior of Solids*, editor, M. Kanninen, et al., McGraw-Hill, New York (1970).

10. J. H. Evans, "Structural Analysis of Shipping Casks, Vol. 8, Experimental Study of the Stress-Strain Properties of Lead Under Specified Impact Conditions," ORNL-TM-1312, Oak Ridge National Laboratory, Oak Ridge, TN (August 1970).

11. J. Duffy, R. H. Hawley, and R. A. Frantz, Jr., "The Deformation of Lead in Torsion at High Rates," *J. of Appl. Mech.*, p. 651 (1972).

12. P. V. Marcal, "A Stiffness Method for Elastic-Plastic Problems," *Int. J. Mech. Sci.*, Vol. 7, pp. 229-238 (1965).

13. P. V. Marcal and W. R. Pilgrim, "A Stiffness Method for Elastic-Plastic Shells of Revolution," Pressure Vessel and Piping: Design and Analysis, Vol. 1, Analysis, G. J. Bohm, editor, The Amer. Soc. of Mech. Engrs., New York (1972). (Reprint from *J. of Strain Analysis*, Instn. of Mech. Engrs, 1966)

14. R. J. Roark and W. C. Young, Formulas for Stress and Strain, McGraw-Hill Book Co. (1975).

15. J. O. Hallquist, "NIKE2D - A Vectorized, Implicit Finite Deformation Finite Element Code for Analyzing the Static and Dynamic Response of 2-D Solids with Interactive Re-zoning and Graphics," Lawrence Livermore National Laboratory, UCID-19677, Rev. 1, December 1986.

16. G. C. Mok and M. C. Witte, "The Use of SCANS for Impact Studies of Transportation Packages," 29th Annual Meeting Proceedings, Institute of Nuclear Materials Management, June 26-29, 1988, Las Vegas, NV, p. 160.

17. "Consolidated Safety Analysis Report for IF300 Shipping Cask," General Electric Nuclear Energy Division Report NEDO-10084, San Jose, CA, September 1984.

18. L. B. Shappert, et al., "A Guide for the Design, Fabrication, and Operation of Shipping Casks for Nuclear Applications," Oak Ridge National Laboratory Report ORNL-NSIC-68, Oak Ridge, TN, February 1970.

APPENDIX A

SCANS' Input for Verification Problems

A.1 SCANS Input for Sample Problems

Figures A-1-1 through A-5-2 are a copy of SCANS input pages for Sample Problems 1 through 5. These pages contain all the required input values to define the basic geometry of the cask and the force-deformation relation of the impact limiters. From these pages, the user can identify the exact input values and reproduce the results presented in this report for Sample Problems 1 through 5. Only the pages that are essential for the impact analyses are shown. These pages also contain some default values that are automatically created by the program and some input values that are used for other but not the impact analyses. Input values entered on other pages but not shown herein might be required by the program, but they will have no effect on the results of the impact analyses.

```
Basic Geometry Specifications                    ID:0001           Today is: 5/16/91
 General SAR Information                         Page 1   of 12  Last chgd:11/17/88
-----------------------------------------------------------------------------------
SAR title....[Prob. 1, Rail Cask w/ Solid Caps & Soft Limiters         ]

SAR docket number...........[        ]   SAR report number........[             ]

SAR docket start date.......[8/12/88 ]   SAR report date..........[        ]

Add. info....[                                                          ]

Add. info....[                                                          ]

Add. info....[                                                          ]

Comp addr....[                                                          ]

Comp addr....[                                                          ]

Comp addr....[                                                          ]
-----------------------------------------------------------------------------------
```

```
Basic Geometry Specifications                    ID:0001           Today is: 5/16/91
 Cask Cavity/Contents Specifications             Page 3   of 12  Last chgd: 5/27/88
-----------------------------------------------------------------------------------
Cavity inner radius (in.)...................................[30.          ]
Cavity length (in.).........................................[179.         ]

Gross weight of package (lbs)...............................[196878.      ]
Weight of contents / internals (lbs)........................[52000.       ]

Maximum heat generation rate of contents (Btu/min)..........[0.           ]

Initial cavity charge pressure (psia).......................[14.7         ]
Initial cavity charge temperature (deg.F)...................[70.          ]
Maximum normal operating pressure (psia)....................[14.7         ]

Temperature defining stress free condition (deg.F)..........[70.          ]

(Include the following to define 2-D finite-element mesh)
            (Mesh divisions must be even)

Number of mesh divisions along cavity inner radius.........[6 ]
Number of mesh divisions along cavity half length..........[8 ]
-----------------------------------------------------------------------------------
```

```
Basic Geometry Specifications                    ID:0001           Today is: 5/16/91
 Cask Component Configurations                   Page 4   of 12  Last chgd:11/17/88
-----------------------------------------------------------------------------------
Shell configuration..................[L]
    (S=solid, L=laminated)

Top end cap configuration............[S]
    (S=solid, L=laminated)

Bottom end cap configuration.........[S]
    (S=solid, L=laminated)


Is Top impact limiter present?              [Y/N]........[Y]

Is Bottom impact limiter present?           [Y/N]........[Y]

Is Neutron shield / water jacket present? [Y/N]........[N]

-----------------------------------------------------------------------------------
```

```
Basic Geometry Specifications                    ID:0001           Today is: 5/16/91
 Cask Shell Specifications (LAMINATED)           Page 5b  of 12  Last chgd: 8/24/87
-----------------------------------------------------------------------------------
Shell inner  layer thickness (in.)....................[1.5          ]
 Additional thickness at end cap interface (in.)...[0.           ]
Shell inner  layer material name......................[SS304    ]

Shell shield layer thickness (in.)....................[4.           ]
Shell shield length (in.).............................[179.         ]
Shell shield layer material name......................[LEAD     ]

Shell outer  layer thickness (in.)....................[2.5          ]
 Additional thickness at end cap interface (in.)...[0.           ]
Shell outer  layer material name......................[SS304    ]


(Include the following to define 2-D finite-element mesh)
            (Mesh divisions must be even)

Number of mesh divisions through shell inner  layer...........[2 ]
Number of mesh divisions through shell shield layer...........[4 ]
Number of mesh divisions through shell outer  layer...........[2 ]
-----------------------------------------------------------------------------------
```

Figure A-I-1 SCANS input pages for basic geometry of Sample Problem 1.

```
Basic Geometry Specifications                   ID:0001          Today is: 5/16/91
 Cask Top End Cap Specifications (SOLID)        Page 6a   of 12  Last chgd: 8/24/87
----------------------------------------------------------------------------------
End cap thickness (in.).......[7.          ]

End cap material name.........[SS304   ]


(Include the following to define 2-D finite-element mesh)
              (Mesh divisions must be even)

Number of mesh divisions through end cap....[4 ]


Press  F10  to copy data from other end cap (if it is SOLID)
----------------------------------------------------------------------------------
```

```
Basic Geometry Specifications                   ID:0001          Today is: 5/16/91
 Cask Bottom End Cap Specifications (SOLID)     Page 7a   of 12  Last chgd: 8/24/87
----------------------------------------------------------------------------------
End cap thickness (in.).......[7.          ]

End cap material name.........[SS304   ]


(Include the following to define 2-D finite-el. ent mesh)
              (Mesh divisions must be even)

Number of mesh divisions through end cap....[4 ]


Press  F10  to copy data from other end cap (if it is SOLID)
----------------------------------------------------------------------------------
```

```
Basic Geometry Specifications                   ID:0001          Today is: 5/16/91
 Cask Closure Bolts Information                 Page 8    of 12  Last chgd: 8/24/87
----------------------------------------------------------------------------------
Number of closure bolts..............................[20]

Diameter of closure bolts (in.)......................[1.          ]

Closure bolt circle radius (in.).....................[37.         ]
----------------------------------------------------------------------------------
```

```
Basic Geometry Specifications                   ID:0001          Today is: 5/16/91
 Cask Impact Model Specifications               Page 12   of 12  Last chgd: 6/17/88
----------------------------------------------------------------------------------
Number of elements for 1-D impact model.......[8 ]
TOP Impact limiter weight (lbs)...............[11212.      ]
BOTTOM Impact limiter weight (lbs)............[11212.      ]
(If omitted, weights are calculated based on volume and density)

Define impact model with user specified properties? (Y/N).......[N]
----------------------------------------------------------------------------------
```

Figure A-1-1 SCANS input pages for basic geometry of Sample Problem 1. (Continued)

```
Impact Limiter Deflection/Force Data          ID:0001          Today is: 5/16/91
 Impact Limiter Unloading Specification       Page 0    of 2h  Last chgd: 8/24/87
-----------------------------------------------------------------------------------

   Select the slope of the unloading path for impact limiters

     C -- Unloading slope is maximum slope of limiter curve
     N -- No elastic recovery of impact limiter
           (Approximated by unloading slope of 5 times max slope of curve)
     U -- User specified unloading slope

   Type of Impact Limiter Unloading..............[N]

-----------------------------------------------------------------------------------
```

```
Impact Limiter Deflection/Force Data          ID:0001          Today is: 5/16/91
 Bottom Impact Limiter for 0 degree impact    Page 1a   of 2h  Last chgd:11/17/88
-----------------------------------------------------------------------------------
Press  F10  to copy Force/Deflection data from another impact angle

Impact angle is defined as follows:  SIDE impact angle is 0.
                                   END ON impact angle is 90.

Do you wish to define a Deflection/Force curve for this angle ? [Y/N].......[Y]

              You must define at least 2 deflection/force pairs
    Deflection #0  (in)     .0                 Force #0  (kips)     .0
    Deflection #1  (in)...[.3          ]       Force #1  (kips)...[10.          ]
    Deflection #2  (in)...[3.          ]       Force #2  (kips)...[100.         ]
    Deflection #3  (in)...[0.          ]       Force #3  (kips)...[0.           ]
    Deflection #4  (in)...[0.          ]       Force #4  (kips)...[0.           ]
    Deflection #5  (in)...[0.          ]       Force #5  (kips)...[0.           ]
    Deflection #6  (in)...[0.          ]       Force #6  (kips)...[0.           ]
    Deflection #7  (in)...[0.          ]       Force #7  (kips)...[0.           ]
    Deflection #8  (in)...[0.          ]       Force #8  (kips)...[0.           ]
    Deflection #9  (in)...[0.          ]       Force #9  (kips)...[0.           ]
    Deflection #10 (in)...[0.          ]       Force #10 (kips)...[0.           ]
-----------------------------------------------------------------------------------
```

Figure A-1-2 SCANS input pages for limiter force-deformation relation of Sample Problem 1. The input for all impact angles are identical; therefore, only the page for 0-degree impact is shown herein.

```
Basic Geometry Specifications                    ID:0002          Today is: 5/14/91
 General SAR Information                         Page 1   of 12  Last chgd:11/16/88
-----------------------------------------------------------------------------------
SAR title....[Prob. 2, Rail Cask w/ Laminated Caps & Soft Limiters  ]

SAR docket number............[       ]  SAR report number.......[             ]

SAR docket start date.......[10/17/88]  SAR report date..........[         ]

Add. info....[                                                      ]

Add. info....[                                                      ]

Add. info....[                                                      ]

Comp addr....[                                                      ]

Comp addr....[                                                      ]

Comp addr....[                                                      ]
-----------------------------------------------------------------------------------
```

```
Basic Geometry Specifications                    ID:0002          Today is: 5/16/91
 Cask Component Configurations                   Page 4   of 12  Last chgd:11/17/88
-----------------------------------------------------------------------------------
Shell configuration.................[L]
    [S=solid, L=laminated]

Top end cap configuration...........[L]
    [S=solid, L=laminated]

Bottom end cap configuration........[L]
    [S=solid, L=laminated]


Is Top impact limiter present?             [Y/N]........[Y]

Is Bottom impact limiter present?          [Y/N]........[Y]

Is Neutron shield / water jacket present? [Y/N]........[N]

-----------------------------------------------------------------------------------
```

```
Basic Geometry Specifications                    ID:0002          Today is: 5/16/91
 Cask Bottom End Cap Specs (LAMINATED)           Page 7b  of 12  Last chgd:10/12/88
-----------------------------------------------------------------------------------
End cap inner layer thickness (in)...........[1.5          ]
End cap inner layer material name............[SS304    ]

End cap shield layer thickness (in.).........[6.           ]
End cap shield layer radius (in.)............[35.5         ]
End cap shield layer material name...........[LEAD     ]

End cap outer layer thickness (in.)..........[2.5          ]
End cap outer layer material name............[SS304    ]

(Include the following to define 2-D finite-element mesh)
           (Mesh divisions must be even)

Number of mesh divisions through end cap inner layer.........[2 ]
Number of mesh divisions through end cap shield layer........[4 ]
Number of mesh divisions through end cap outer layer.........[2 ]


Press  F10  to copy data from other end cap (if it is LAMINATED)
-----------------------------------------------------------------------------------
```

Figure A-2-1 SCANS input pages for basic geometry of Sample Problem 2. Other required pages not shown herein are identical to those of Sample Problem 1 (Fig. A-1-1).

```
Impact Limiter Deflection/Force Data            ID:0002          Today is: 5/16/91
 Impact Limiter Unloading Specification         Page 0    of 2h  Last chgd: 8/24/87

   Select the slope of the unloading path for impact limiters

     C -- Unloading slope is maximum slope of limiter curve
     N -- No elastic recovery of impact limiter
          (Approximated by unloading slope of 5 times max slope of curve)
     U -- User specified unloading slope

   Type of Impact Limiter Unloading..............[N]
```

```
Impact Limiter Deflection/Force Data            ID:0002          Today is: 5/16/91
 Bottom Impact Limiter for 0 degree impact      Page 1a   of 2h  Last chgd:11/17/88

Press  F10  to copy Force/Deflection data from another impact angle

Impact angle is defined as follows:  SIDE impact angle is 0.
                                     END ON impact angle is 90.

Do you wish to define a Deflection/Force curve for this angle ? [Y/N].......[Y]

               You must define at least 2 deflection/force pairs
    Deflection #0  (in)      .0                  Force #0  (kips)      .0
    Deflection #1  (in)...[.3               ]    Force #1  (kips)...[10.             ]
    Deflection #2  (in)...[3.               ]    Force #2  (kips)...[100.            ]
    Deflection #3  (in)...[0.               ]    Force #3  (kips)...[0.              ]
    Deflection #4  (in)...[0.               ]    Force #4  (kips)...[0.              ]
    Deflection #5  (in)...[0.               ]    Force #5  (kips)...[0.              ]
    Deflection #6  (in)...[0.               ]    Force #6  (kips)...[0.              ]
    Deflection #7  (in)...[0.               ]    Force #7  (kips)...[0.              ]
    Deflection #8  (in)...[0.               ]    Force #8  (kips)...[0.              ]
    Deflection #9  (in)...[0.               ]    Force #9  (kips)...[0.              ]
    Deflection #10 (in)...[0.               ]    Force #10 (kips)...[0.              ]
```

Figure A-2-2 SCANS input pages for limiter force-deformation relation of Sample Problem 2. The input for all impact angles are identical; therefore, only the page for 0-degree impact is shown herein.

```
Basic Geometry Specifications                     ID:0003          Today is: 5/16/91
 General SAR Information                          Page 1   of 12   Last chgd:11/16/88
---------------------------------------------------------------------------------------
SAR title....[Prob. 3, Rail Cask w/ Unboned Shield & Typical Limiter]

SAR docket number...........[        ]  SAR report number.......[              ]

SAR docket start date.......[7/25/88 ]  SAR report date.........[         ]

Add. info....[                                                ]

Add. info....[                                                ]

Add. info....[                                                ]

Comp addr....[                                                ]

Comp addr....[                                                ]

Comp addr....[                                                ]
---------------------------------------------------------------------------------------
```

Figure A-3-1 SCANS input pages for basic geometry of Sample Problem 3. All other input pages for this problem and for Problem 1 are identical.

```
Impact Limiter Deflection/Force Data           ID:0003            Today is: 5/16/91
 Impact Limiter Unloading Specification        Page 0    of 2h  Last chgd: 8/24/87

   Select the slope of the unloading path for impact limiters

     C -- Unloading slope is maximum slope of limiter curve
     N -- No elastic recovery of impact limiter
          (Approximated by unloading slope of 5 times max slope of curve)
     U -- User specified unloading slope

   Type of Impact Limiter Unloading..............[N]
```

```
Impact Limiter Deflection/Force Data           ID:0003            Today is: 5/16/91
 Bottom Impact Limiter for 90 degree impact    Page 1g   of 2h  Last chgd:11/17/88

Press  F10  to copy Force/Deflection data from another impact angle

Impact angle is defined as follows:  SIDE impact angle is 0.
                                     END ON impact angle is 90.

Do you wish to define a Deflection/Force curve for this angle ? [Y/N].......[Y]

                You must define at least 2 deflection/force pairs
    Deflection #0  (in)     .0                   Force #0  (kips)     .0
    Deflection #1  (in)...[.65            ]      Force #1  (kips)...[1680.           ]
    Deflection #2  (in)...[20.            ]      Force #2  (kips)...[2800.           ]
    Deflection #3  (in)...[25.            ]      Force #3  (kips)...[5610.           ]
    Deflection #4  (in)...[30.            ]      Force #4  (kips)...[17400.          ]
    Deflection #5  (in)...[0.             ]      Force #5  (kips)...[0.              ]
    Deflection #6  (in)...[0.             ]      Force #6  (kips)...[0.              ]
    Deflection #7  (in)...[0.             ]      Force #7  (kips)...[0.              ]
    Deflection #8  (in)...[0.             ]      Force #8  (kips)...[0.              ]
    Deflection #9  (in)...[0.             ]      Force #9  (kips)...[0.              ]
    Deflection #10 (in)...[0.             ]      Force #10 (kips)...[0.              ]
```

Figure A-3-2 SCANS input pages for limiter force-deformation relation of Sample Problem 3.

```
Basic Geometry Specifications                  ID:0004          Today is: 5/16/91
 General SAR Information                       Page 1   of 12  Last chgd:11/16/88
---------------------------------------------------------------------------------
SAR title....[Prob. 4, Hallam Cask for Comparison with ORNL Test      ]

SAR docket number...........[        ]  SAR report number.......[              ]

SAR docket start data.......[8/13/88 ]  SAR report date.........[          ]

Add. info....[Cask's Geometry and test results are in ORNL report     ]

Add. info....[NSIC-68, "A Guide for the Design, Fabrication, and      ]

Add. info....[Operation of Shipping Casks for Nuclear Applications"   ]

Comp addr....[                                                         ]

Comp addr....[                                                         ]

Comp addr....[                                                         ]
---------------------------------------------------------------------------------
```

```
Basic Geometry Specifications                  ID:0004          Today is: 5/16/91
 Cask Cavity/Contents Specifications           Page 3   of 12  Last chgd:11/19/87
---------------------------------------------------------------------------------
Cavity inner radius (in.)...............................[1.2175          ]
Cavity length (in.).....................................[27.07812        ]

Gross weight of package (lbs)...........................[165.            ]
Weight of contents / internals (lbs)....................[1.              ]

Maximum heat generation rate of contents (Btu/min)......[0.              ]

Initial cavity charge pressure (psia)...................[14.7            ]
Initial cavity charge temperature (deg.F)...............[70.             ]
Maximum normal operating pressure (psia)................[14.7            ]

Temperature defining stress free condition (deg.F)......[70.             ]

(Include the following to define 2-D finite-element mesh)
            (Mesh divisions must be even)

Number of mesh divisions along cavity inner radius.......[6 ]
Number of mesh divisions along cavity half length........[8 ]
---------------------------------------------------------------------------------
```

```
Basic Geometry Specifications                  ID:0004          Today is: 5/16/91
 Cask Component Configurations                 Page 4   of 12  Last chgd:11/17/89
---------------------------------------------------------------------------------
Shell configuration.................[L]
    [S=solid, L=laminated]

Top end cap configuration...........[S]
    [S=solid, L=laminated]

Bottom end cap configuration........[S]
    [S=solid, L=laminated]


Is Top impact limiter present?             [Y/N]........[Y]

Is Bottom impact limiter present?          [Y/N]........[Y]

Is Neutron shield / water jacket present?  [Y/N]........[N]
---------------------------------------------------------------------------------
```

```
Basic Geometry Specifications                  ID:0004          Today is: 5/16/91
 Cask Shell Specifications (LAMINATED)         Page 5b  of 12  Last chgd:11/19/87
---------------------------------------------------------------------------------
Shell inner  layer thickness (in.)....................[.0950000        ]
 Additional thickness at end cap interface (in.)....[0.              ]
Shell inner  layer material name......................[SS304    ]

Shell shield layer thickness (in.)....................[.936            ]
Shell shield length (in.).............................[27.07812        ]
Shell shield layer material name......................[LEAD     ]

Shell outer  layer thickness (in.)....................[.202            ]
 Additional thickness at end cap interface (in.)....[0.              ]
Shell outer  layer material name......................[SS304    ]


(Include the following to define 2-D finite-element mesh)
            (Mesh divisions must be even)

Number of mesh divisions through shell inner  layer...........[2 ]
Number of mesh divisions through shell shield layer...........[4 ]
Number of mesh divisions through shell outer  layer...........[2 ]
---------------------------------------------------------------------------------
```

Figure A-4-1 SCANS input pages for basic geometry of Sample Problem 4.

```
Basic Geometry Specifications                    ID:0004           Today is: 5/16/91
 Cask Top End Cap Specifications (SOLID)         Page 6a   of 12  Last chgd:11/19/87
------------------------------------------------------------------------------------
End cap thickness (in.)........[.25          ]

End cap material name..........[SS304   ]



(Include the following to define 2-D finite-element mesh)
          (Mesh divisions must be even)

Number of mesh divisions through end cap....[4 ]



Press  F10  to copy data from other end cap (if it is SOLID)

------------------------------------------------------------------------------------
```

```
Basic Geometry Specifications                    ID:0004           Today is: 5/16/91
 Cask Bottom End Cap Specifications (SOLID)      Page 7a   of 12  Last chgd:11/19/87
------------------------------------------------------------------------------------
End cap thickness (in.)........[.25          ]

End cap material name..........[SS304   ]



(Include the following to define 2-D finite-element mesh)
          (Mesh divisions must be even)

Number of mesh divisions through end cap....[4 ]



Press  F10  to copy data from other end cap (if it is SOLID)

------------------------------------------------------------------------------------
```

```
Basic Geometry Specifications                    ID:0004           Today is: 5/16/91
 Cask Closure Bolts Information                  Page 8    of 12  Last chgd:11/19/87
------------------------------------------------------------------------------------
Number of closure bolts............................[8 ]

Diameter of closure bolts (in.)....................[.25          ]

Closure bolt circle radius (in.)...................[2.           ]

------------------------------------------------------------------------------------
```

```
Basic Geometry Specifications                    ID:0004           Today is: 5/16/91
 Cask Impact Model Specifications                Page 12   of 12  Last chgd:11/17/88
------------------------------------------------------------------------------------
Number of elements for 1-D impact model........[17 ]
TOP Impact limiter weight (lbs)................[6.65          ]
BOTTOM Impact limiter weight (lbs).............[6.65          ]
(If omitted, weights are calculated based on volume and density)

Define impact model with user specified properties? [Y/N]........[N]

------------------------------------------------------------------------------------
```

Figure A-4-1 SCANS input pages for basic geometry of Sample Problem 4. (Continued)

```
Impact Limiter Deflection/Force Data            ID:0004          Today is: 5/16/91
 Impact Limiter Unloading Specification         Page 0   of 2h  Last chgd:11/17/86

   Select the slope of the unloading path for impact limiters

      C -- Unloading slope is maximum slope of limiter curve
      N -- No elastic recovery of impact limiter
           (Approximated by unloading slope of 5 times max slope of curve)
      U -- User specified unloading slope

   Type of Impact Limiter Unloading..............[N]
```

```
Impact Limiter Deflection/Force Data            ID:0004          Today is: 5/16/91
 Bottom Impact Limiter for 90 degree impact     Page 1g  of 2h  Last chgd: 8/13/88

Press  F10  to copy Force/Deflection data from another impact angle

Impact angle is defined as follows:  SIDE impact angle is 0.
                                     END ON impact angle is 90.

Do you wish to define a Deflection/Force curve for this angle ? [Y/N].......[Y]

            You must define at least 2 deflection/force pairs
     Deflection #0  (in)     .0                 Force #0  (kips)     .0
     Deflection #1  (in)...[1.           ]      Force #1  (kips)...[258500.      ]
     Deflection #2  (in)...[2.           ]      Force #2  (kips)...[517000.      ]
     Deflection #3  (in)...[0.           ]      Force #3  (kips)...[0.           ]
     Deflection #4  (in)...[0.           ]      Force #4  (kips)...[0.           ]
     Deflection #5  (in)...[0.           ]      Force #5  (kips)...[0.           ]
     Deflection #6  (in)...[0.           ]      Force #6  (kips)...[0.           ]
     Deflection #7  (in)...[0.           ]      Force #7  (kips)...[0.           ]
     Deflection #8  (in)...[0.           ]      Force #8  (kips)...[0.           ]
     Deflection #9  (in)...[0.           ]      Force #9  (kips)...[0.           ]
     Deflection #10 (in)...[0.           ]      Force #10 (kips)...[0.           ]
```

Figure A-4-2 SCANS input pages for limiter force-deformation relation of Sample Problem 4.

```
Basic Geometry Specifications                          ID:0005            Today is: 5/16/91
 Cask Cavity/Contents Specifications                   Page 3   of 12  Last chgd: 9/18/87
--------------------------------------------------------------------------------------------
Cavity inner radius (in.)...............................[18.75          ]
Cavity length (in.).....................................[182.25         ]

Gross weight of package (lbs)...........................[131822.        ]
Weight of contents / internals (lbs)....................[22472.         ]

Maximum heat generation rate of contents (Btu/min)......[4367.          ]

Initial cavity charge pressure (psia)...................[14.7           ]
Initial cavity charge temperature (deg.F)...............[70.            ]
Maximum normal operating pressure (psia)................[400.           ]

Temperature defining stress free condition (deg.F)......[70.            ]

(Include the following to define 2-D finite-element mesh)
          (Mesh divisions must be even)

Number of mesh divisions along cavity inner radius.......[6 ]
Number of mesh divisions along cavity half length........[8 ]
--------------------------------------------------------------------------------------------
```

```
Basic Geometry Specifications                          ID:0005            Today is: 5/16/91
 Cask Component Configurations                         Page 4   of 12  Last chgd:11/17/88
--------------------------------------------------------------------------------------------
Shell configuration.................[L]
    [S=solid, L=laminated]

Top end cap configuration...........[L]
    [S=solid, L=laminated]

Bottom end cap configuration........[L]
    [S=solid, L=laminated]


Is Top impact limiter present?             [Y/N].......[Y]

Is Bottom impact limiter present?          [Y/N].......[Y]

Is Neutron shield / water jacket present?  [Y/N].......[Y]


--------------------------------------------------------------------------------------------
```

Figure A-5-1 SCANS input pages for basic geometry of Sample Problem 5.

```
Basic Geometry Specifications                        ID:0005          Today is: 5/16/91
 Cask Shell Specifications (LAMINATED)               Page 5b  of 12   Last chgd: 9/02/87
---------------------------------------------------------------------------------------
Shell inner  layer thickness (in.)...................[.5             ]
 Additional thickness at end cap interface (in.)....[0.             ]
Shell inner  layer material name....................[SS316    ]

Shell shield layer thickness (in.)...................[4.             ]
Shell shield length (in.)............................[182.25         ]
Shell shield layer material name....................[DURANIUM]

Shell outer  layer thickness (in.)...................[1.5            ]
 Additional thickness at end cap interface (in.)....[0.             ]
Shell outer  layer material name....................[SS316    ]


(Include the following to define 2-D finite-element mesh)
            (Mesh divisions must be even)

Number of mesh divisions through shell inner  layer...........[2 ]
Number of mesh divisions through shell shield layer...........[4 ]
Number of mesh divisions through shell outer  layer...........[2 ]
---------------------------------------------------------------------------------------
```

```
Basic Geometry Specifications                        ID:0005          Today is: 5/16/91
 Cask Top End Cap Specifications (LAMINATED)         Page 6b  of 12   Last chgd: 9/02/87
---------------------------------------------------------------------------------------
End cap inner layer thickness (in).........[1.5            ]
End cap inner layer material name..........[SS304    ]

End cap shield layer thickness (in.).......[3.75           ]
End cap shield layer radius (in.)..........[20.            ]
End cap shield layer material name.........[DURANIUM]

End cap outer layer thickness (in.) .......[1.25           ]
End cap outer layer material name..........[SS304    ]

(Include the following to define 2-D finite-element mesh)
            (Mesh divisions must be even)

Number of mesh divisions through end cap inner layer.........[2 ]
Number of mesh divisions through end cap shield layer........[4 ]
Number of mesh divisions through end cap outer layer.........[2 ]

Press  F10  to copy data from other end cap (if it is LAMINATED)
---------------------------------------------------------------------------------------
```

Figure A-5-1 SCANS input pages for basic geometry of Sample Problem 5. (Continued)

```
Basic Geometry Specifications                       ID:0005          Today is: 5/16/91
 Cask Bottom End Cap Specs (LAMINATED)              Page 7b  of 12  Last chgd: 9/02/87
=====================================================================================
End cap inner layer thickness (in)..........[1.5          ]
End cap inner layer material name...........[SS304    ]

End cap shield layer thickness (in.)........[3.75         ]
End cap shield layer radius (in.)...........[20.          ]
End cap shield layer material name..........[DURANIUM]

End cap outer layer thickness (in.).........[1.25         ]
End cap outer layer material name...........[SS304    ]

(Include the following to define 2-D finite-element mesh)
          (Mesh divisions must be even)

Number of mesh divisions through end cap inner layer.........[2 ]
Number of mesh divisions through end cap shield layer........[4 ]
Number of mesh divisions through end cap outer layer.........[2 ]

Press  F10  to copy data from other end cap (if it is LAMINATED)
=====================================================================================
```

```
Basic Geometry Specifications                       ID:0005          Today is: 5/16/91
 Cask Impact Model Specifications                   Page 12  of 12  Last chgd:11/17/88
=====================================================================================
Number of elements for 1-D impact model.......[10]
TOP Impact limiter weight (lbs)...............[3846.        ]
BOTTOM Impact limiter weight (lbs)............[3846.        ]
(If omitted, weights are calculated based on volume and density)

Define impact model with user specified properties? [Y/N].......[N]




=====================================================================================
```

Figure A-5-1 SCANS input pages for basic geometry of Sample Problem 5. (Continued)

```
Impact Limiter Deflection/Force data              ID:0005            Today is: 5/16/91
 Impact Limiter Unloading Specification           Page 0    of 2h   Last chgd: 9/02/87
--------------------------------------------------------------------------------------

   Select the slope of the unloading path for impact limiters

     C -- Unloading slope is maximum slope of limiter curve
     N -- No elastic recovery of impact limiter
          (Approximated by unloading slope of 5 times max slope of curve)
     U -- User specified unloading slope

   Type of Impact Limiter Unloading..............[N]

--------------------------------------------------------------------------------------
```

```
Impact Limiter Deflection/Force Data              ID:0005            T day is: 5/16/91
 Bottom Impact Limiter for 0 degree impact        Page 1a   of 2h   Last chgd:11/17/88
--------------------------------------------------------------------------------------
Press  F10  to copy Force/Deflection data from another impact angle

Impact angle is defined as follows:  SIDE impact angle is 0
                                     END ON impact angle is 90.

Do you wish to define a Deflection/Force curve for this angle ? [Y/N].......[Y]

                You must define at least 2 deflection/force pairs
   Deflection #0  (in)     .0                         Force #0  (kips)     .0
   Deflection #1  (in)...[.316         ]              Force #1  (kips)...[14110.      ]
   Deflection #2  (in)...[.501         ]              Force #2  (kips)...[6360.       ]
   Deflection #3  (in)...[10.          ]              Force #3  (kips)...[6360.       ]
   Deflection #4  (in)...[0.           ]              Force #4  (kips)...[0.          ]
   Deflection #5  (in)...[0.           ]              Force #5  (kips)...[0.          ]
   Deflection #6  (in)...[0.           ]              Force #6  (kips)...[0.          ]
   Deflection #7  (in)...[0.           ]              Force #7  (kips)...[0.          ]
   Deflection #8  (in)...[0.           ]              Force #8  (kips)...[0.          ]
   Deflection #9  (in)...[0.           ]              Force #9  (kips)...[0.          ]
   Deflection #10 (in)...[0.           ]              Force #10 (kips)...[0.          ]
--------------------------------------------------------------------------------------
```

```
Impact Limiter Deflection/Force Data              ID:0005            Today is: 5/1./91
 Bottom Impact Limiter for 90 degree impact       Page 1g   of 2h   Last chgd:11/17/88
--------------------------------------------------------------------------------------
Press  F10  to copy Force/Deflection data from another impact angle

Impact angle is defined as follows:  SIDE impact angle is 0.
                                     END ON impact angle is 90.

Do you wish to define a Deflection/Force curve for this angle ? [Y/N].......[Y]

                You must define at least 2 deflection/force pairs
   Deflection #0  (in)     .0                         Force #0  (kips)     .0
   Deflection #1  (in)...[.158         ]              Force #1  (kips)...[40140.      ]
   Deflection #2  (in)...[.253         ]              Force #2  (kips)...[17840.      ]
   Deflection #3  (in)...[10.          ]              Force #3  (kips)...[17840.      ]
   Deflection #4  (in)...[0.           ]              Force #4  (kips)...[0.          ]
   Deflection #5  (in)...[0.           ]              Force #5  (kips)...[0.          ]
   Deflection #6  (in)...[0.           ]              Force #6  (kips)...[0.          ]
   Deflection #7  (in)...[0.           ]              Force #7  (kips)...[0.          ]
   Deflection #8  (in)...[0.           ]              Force #8  (kips)...[0.          ]
   Deflection #9  (in)...[0.           ]              Force #9  (kips)...[0.          ]
   Deflection #10 (in)...[0.           ]              Force #10 (kips)...[0.          ]
--------------------------------------------------------------------------------------
```

Figure A-5-2 SCANS input pages for limiter force-deformation relation of Sample Problem 5.

APPENDIX B

Additional Comparison of SCANS Results

(Sample Problems 1 and 2)

Appendix B presents verification results that are omitted in Chapter 6 of this report. The results are for the Sample Problems 1 and 2 defined in Chapter 6. The casks used for the two problems differ only in the end caps and in the impact limiter. As depicted in Fig. 6-1 of Chapter 6, all the casks have the dimensions of a typical rail cask. The casks for Problem 1 have two identical solid end caps, but the cask for Problem 2 has two unequal laminated end caps of slightly different thickness of the lead shield. The same limiter force-deformation relation is used for Problems 1 and 2.

Problem 1 was employed to verify all printed output of SCANS quasi-static and dynamic analysis options. Supplementing Problem 1, Problem 2 was used to check the calculation of stresses in the laminated end caps.

The results of Problem 1 presented in this appendix include all the maximum stresses in the cask body, the end caps, and the top closure bolts generated by a 30-ft drop. For the cask body, the maximum axial force, shear force, and bending moment are also presented for various axial locations of the cask (Tables B-1 through B-4). The cask stresses are tabulated for a side drop (Table B-5), a 45-degree oblique drop (Table B-6), an end drop (Table B-7), and a C.G. drop (Table B-8). The end cap and bolt stresses are listed for both bottom and top impacts at four other oblique angles in addition to the foregoing ones (Tables B-9-1 through B-12). The stresses in the laminated end caps of Sample Problem 2 are tabulated in Tables B-13-1 and B-13-2.

Table B-1

Comparison of SCANS Results for Forces and Moments in a Cask Undergoing a 30 Ft. Side Drop (Sample Problem 1)

Distance from Impact End	Maximum Axial Force (kip)			Maximum Shear Force (kip)			Max. Bending Moment (in-kip)		
	Quasi-static		Dynamic	Quasi-static		Dynamic	Quasi-static		Dynamic
(in)	Hand Calc	SCANS	SCANS	Hand Calc	SCANS	SCANS	Hand Calc	SCANS	SCANS
0.0	0.0	0.0	0.5	1070.1	1070.1	1150.4	5379.7	5379.7	5816.8
22.4	0.0	0.0	0.4	917.2	917.2	987.7	29323.1	29322.9	31578.7
44.8	0.0	0.0	0.2	611.5	611.5	661.0	46425.5	46425.1	50074.8
67.1	0.0	0.0	0.1	305.7	305.7	331.8	56686.9	56686.5	61202.7
89.5	0.0	0.0	0.0	0.0	0.0	0.0	60107.4	60106.9	64924.7
111.9	0.0	0.0	0.1	-305.7	-305.7	-331.8	56686.9	56686.5	61202.7
134.3	0.0	0.0	0.2	-611.5	-611.5	-661.0	46425.5	46425.1	50074.8
156.6	0.0	0.0	0.4	-917.2	-917.2	-987.7	29323.1	29322.9	31578.7
179.0	0.0	0.0	0.5	-1070.1	-1070.1	-1150.4	5379.7	5379.7	5816.8

Table D-2

Comparison of SCANS Results for Forces and Moments in a Cask Undergoing a 30 Ft. 45 Degree Oblique Drop (Sample Problem 1)

Distance from Impact End	Maximum Axial Force (kip)			Maximum Shear Force (kip)			Max. Bending Moment (in-kip)		
	Quasi-static		Dynamic	Quasi-static		Dynamic	Quasi-static		Dynamic
(in)	Hand Calc	SCANS	SCANS	Hand Calc	SCANS	SCANS	Hand Calc	SCANS	SCANS
0	-1226.6	-1226.6	-895.9	951.6	951.6	962.9	-45683.1	-45682.9	-33405.9
22.375	-1154.7	-1154.7	-831.8	812.1	812.1	795.9	-24782.5	-24782.4	-15574.2
44.75	-1010.9	-1010.9	-709.7	555.7	555.7	493.1	-10513.8	-10513.9	10157.7
67.125	-867.0	-867.0	-595.1	344.3	344.3	266.0	-1478.6	-1478.7	14920.2
89.5	-723.2	-723.2	509.5	178.0	178.0	113.2	3330.6	3330.4	15956.2
111.875	-579.3	-579.3	488.5	56.6	56.6	-102.6	4921.2	4921.0	13722.7
134.25	-435.5	-435.5	425.9	-19.7	-19.7	-155.8	4300.6	4300.3	9588.1
156.625	-291.6	-291.6	321.1	-51.0	-51.0	-155.0	2476.1	2475.9	4780.6
179	-219.7	-219.7	258.0	-55.4	-55.4	-139.6	846.4	846.1	1195.2

Table 8-3

Comparison of SCANS Results for Forces and Moments in a Cask
Undergoing a 30 Ft. End Drop (Sample Problem 1)

Distance from Impact End	Maximum Axial Force (kip)			Maximum Shear Force (kip)			Max. Bending Moment (in-kip)		
	Quasi-static		Dynamic	Quasi-static		Dynamic	Quasi-static		Dynamic
(in)	Hand Calc	SCANS	SCANS	Hand Calc	SCANS	SCANS	Hand Calc	SCANS	SCANS
0.0	-1843.5	-1843.5	-2022.3	0.0	0.0	0.0	0.0	0.0	0.0
22.4	-1735.4	-1735.4	-1905.0	0.0	0.0	0.0	0.0	0.0	0.0
44.8	-1519.2	-1519.2	-1669.8	0.0	0.0	0.0	0.0	0.0	0.0
67.1	-1303.1	-1303.1	-1433.3	0.0	0.0	0.0	0.0	0.0	0.0
89.5	-1086.9	-1086.9	-1196.6	0.0	0.0	0.0	0.0	0.0	0.0
111.9	-870.7	-870.7	-960.0	0.0	0.0	0.0	0.0	0.0	0.0
134.3	-654.5	-654.5	-722.3	0.0	0.0	0.0	0.0	0.0	0.0
156.6	-438.3	-438.3	-483.6	0.0	0.0	0.0	0.0	0.0	0.0
179.0	-330.2	-330.2	-364.6	0.0	0.0	0.0	0.0	0.0	0.0

Table B-4

Comparison of SCANS Results for Forces and Moments in a Cask
Undergoing a 30 Ft. C.G. Drop (Sample Problem 1)

Distance from Impact End	Maximum Axial Force (kip)			Maximum Shear Force (kip)			Max. Bending Moment (in-kip)		
	Quasi-static		Dynamic	Quasi-static		Dynamic	Quasi-static		Dynamic
(in)	Hand Calc	SCANS	SCANS	Hand Calc	SCANS	SCANS	Hand Calc	SCANS	SCANS
0.0	-1715.3	-1715.3	-1881.7	675.5	675.5	742.0	-71282.1	-71282.1	-78106.4
22.4	-1614.8	-1614.7	-1772.6	635.9	635.9	698.8	-56168.5	-56168.6	-61617.5
44.8	-1413.6	-1413.6	-1553.6	556.6	556.6	611.9	-42827.3	-42827.4	-47077.1
67.1	-1212.4	-1212.4	-1333.6	477.4	477.4	525.0	-31258.5	-31258.6	-34442.2
89.5	-1011.3	-1011.3	-1113.3	398.2	398.2	438.1	-21462.1	-21462.2	-23675.0
111.9	-810.1	-810.1	-893.2	319.0	319.0	351.0	-13438.0	-13438.1	-14889.7
134.3	-609.0	-609.0	-672.0	239.8	239.8	266.4	-7186.3	-7186.4	-8030.5
156.6	-407.8	-407.8	-450.0	160.6	160.6	179.5	-2707.0	-2707.0	-3090.8
179.0	-307.2	-307.2	-339.2	121.0	121.0	135.7	0.0	0.0	115.0

Table 8-5

Comparison of SCANS Results for Stress Intensity in a Cask Undergoing a 30 Ft. Side Drop (Sample Problem 1)

Distance from Impact End (in)	Stress Intensity (psi) Which Corresponds to: Maximum Bending Stress — Quasi-static Hand Calc	Maximum Bending Stress — Quasi-static SCANS	Maximum Bending Stress — Dynamic SCANS	Minimum Bending Stress — Quasi-static Hand Calc	Minimum Bending Stress — Quasi-static SCANS	Minimum Bending Stress — Dynamic SCANS	Maximum Shear — Quasi-static Hand Calc	Maximum Shear — Quasi-static SCANS	Maximum Shear — Dynamic SCANS
Inner Steel Shell									
0.0	291	291	315	291	291	314	4558	4558	4900
22.4	1588	1588	1710	1588	1588	1709	3907	3907	4207
44.8	2514	2514	2712	2514	2514	2711	2605	2605	2816
67.1	3069	3069	3314	3069	3069	3314	1302	1302	1413
89.5	3255	3255	3515	3255	3255	3515	0	0	0
111.9	3069	3069	3314	3069	3069	3314	1302	1302	1413
134.3	2514	2514	2712	2514	2514	2711	2605	2605	2816
156.6	1588	1588	1710	1588	1588	1709	3907	3907	4207
179.0	291	291	315	291	291	314	4558	4558	4900
Lead Shield									
0.0	27	27	29	27	27	29	390	390	419
22.4	148	148	159	148	148	159	334	334	360
44.8	234	234	253	234	234	253	223	223	241
67.1	286	286	309	286	286	309	111	111	121
89.5	303	303	327	303	303	327	0	0	0
111.9	286	286	309	286	286	309	111	111	121
134.3	234	234	253	234	234	253	223	223	241
156.6	148	148	159	148	148	159	334	334	360
179.0	27	27	29	27	27	29	390	390	419
Outer Steel Shell									
0.0	348	348	377	348	348	376	4558	4558	4900
22.4	1898	1898	2044	1898	1898	2043	3907	3907	4207
44.8	3004	3004	3241	3004	3004	3240	2605	2605	2816
67.1	3668	3668	3961	3668	3668	3960	1302	1302	1413
89.5	3890	3890	4201	3890	3890	4201	0	0	0
111.9	3668	3669	3961	3668	3669	3960	1302	1302	1414
134.3	3004	3004	3241	3004	3004	3240	2605	2605	2816
156.6	1898	1898	2044	1898	1898	2043	3907	3907	4207
179.0	348	348	377	348	348	376	4558	4558	4900

Table 8-6

Comparison of SCANS Results for Stress Intensity in a Cask
Undergoing a 30 Ft. · Degree Oblique Drop (Sample Problem 1)

Distance from Impact End (in)	Stress Intensity (psi) Which Corresponds to: Maximum Bending Stress, Quasi-static, Hand Calc	Maximum Bending Stress, Quasi-static, SCANS	Maximum Bending Stress, Dynamic, SCANS	Minimum Bending Stress, Quasi-static, Hand Calc	Minimum Bending Stress, Quasi-static, SCANS	Minimum Bending Stress, Dynamic, SCANS	Maximum Shear, Quasi-static, Hand Calc	Maximum Shear, Quasi-static, SCANS	Maximum Shear, Dynamic, SCANS
Inner Steel Shell									
0.0	1167	1167	861	3780	3780	2762	4259	4259	4177
22.4	112	112	356	2572	2571	1714	3671	3671	3462
44.8	507	507	646	1646	1646	996	2600	2600	2199
67.1	843	843	879	1003	1003	1081	1733	1733	1275
89.5	590	590	947	950	950	1069	1081	1081	699
111.9	350	350	859	883	883	889	662	662	446
134.3	231	231	654	697	697	630	471	471	666
156.6	176	176	410	445	445	355	379	379	661
179.0	188	188	277	280	280	191	332	332	596
Lead Shield									
0.0	119	119	87	342	342	250	364	364	357
22.4	20	20	31	230	230	153	314	314	296
44.8	39	39	59	145	145	87	222	222	188
67.1	71	71	80	86	86	98	148	148	109
89.5	49	49	87	83	83	97	92	92	60
111.9	28	28	78	78	78	81	57	57	38
134.3	18	18	59	61	61	57	40	40	57
156.6	14	14	36	39	39	32	32	32	57
179.0	16	16	24	24	24	17	28	28	51
Outer Steel Shell									
0.0	1650	1650	1213	4262	4262	3115	4259	4259	4177
22.4	374	374	370	2833	2833	1877	3671	3671	3462
44.8	396	396	735	1757	1757	1047	2600	2600	2199
67.1	828	828	1007	1019	1019	1214	1733	1733	1275
89.5	555	555	1097	986	986	1222	1081	1081	699
111.9	298	298	985	935	935	1026	662	662	446
134.3	185	185	740	742	742	715	471	471	666
156.6	150	150	441	471	471	392	379	379	661
179.0	179	179	278	289	289	200	332	332	596

Table 8-7

Comparison of SCANS Results for Stress Intensity in a Cask Undergoing a 30 Ft. End Drop (Sample Problem 1)

Distance from Impact End	Stress Intensity (psi) Which Corresponds to								
	Maximum Bending Stress			Minimum Bending Stress			Maximum Shear		
	Quasi-static		Dynamic	Quasi-static		Dynamic	Quasi-static		Dynamic
(in)	Hand Calc	SCANS	SCANS	Hand Calc	SCANS	SCANS	Hand Calc	SCANS	SCANS
	Inner Steel Shell								
0.0	1963	1963	2153	1963	1963	2153	1963	1963	2153
22.4	1848	1848	2029	1848	1848	2029	1848	1848	2029
44.8	1618	1618	1778	1618	1618	1778	1618	1618	1778
67.1	1388	1388	1526	1388	1388	1526	1388	1388	1526
89.5	1157	1157	1274	1157	1157	1274	1157	1157	1274
111.9	927	927	1022	927	927	1022	927	927	1022
134.3	697	697	769	697	697	769	697	697	769
156.6	467	467	515	467	467	515	467	467	515
179.0	352	[illegible]	388	352	352	388	352	352	388
	Lead Shield								
0.0	168	168	184	168	168	184	168	168	184
22.4	158	158	173	158	158	173	158	158	173
44.8	138	138	152	138	138	152	138	138	152
67.1	119	119	131	119	119	131	119	119	131
89.5	99	99	109	99	99	109	99	99	109
111.9	79	79	87	79	79	87	79	79	87
134.3	60	60	66	60	60	66	60	60	66
156.6	40	40	44	40	40	4	40	40	44
179.0	30	30	33	30	30	33	30	30	33
	Outer Steel Shell								
0.0	1963	1963	2153	1963	1963	2153	1963	1963	2153
22.4	1848	1848	2029	1848	1848	2029	1848	1848	2029
44.8	1618	1618	1778	1618	1618	1778	1618	1618	1778
67.1	1388	1388	1526	1388	1388	1526	1388	1388	1526
89.5	1157	1157	1274	1157	1157	1274	1157	1157	1274
111.9	927	927	1022	927	927	1022	927	927	1022
134.3	697	697	769	697	697	769	697	697	769
156.6	467	467	515	467	467	515	467	467	515
179.0	352	352	388	352	352	388	352	352	388

Table B-8

Comparison of SCANS Results for Stress Intensity in a Cask
Undergoing a 30 Ft. C.G. Drop (Sample Problem 1)

Distance from Impact End (in)	Stress Intensity (psi) Which Corresponds to: Maximum Bending Stress, Quasi-static, Hand Calc	Maximum Bending Stress, Quasi-static, SCANS	Maximum Bending Stress, Dynamic, SCANS	Minimum Bending Stress, Quasi-static, Hand Calc	Minimum Bending Stress, Quasi-static, SCANS	Minimum Bending Stress, Dynamic, SCANS	Maximum Shear, Quasi-static, Hand Calc	Maximum Shear, Quasi-static, SCANS	Maximum Shear, Dynamic, SCANS
Inner Steel Shell									
0.0	2033	2033	2252	5686	5686	6228	3408	3408	3742
22.4	1322	1322	1458	4761	4761	5216	3208	3208	3524
44.8	814	814	906	3824	3824	4192	2809	2809	3081
67.1	401	401	458	2984	2984	3275	2409	2409	2644
89.5	85	85	110	2239	2239	2463	2009	2009	2204
111.9	135	135	9	1590	1590	1754	1610	1610	1770
134.3	259	259	4	1038	1038	1148	1210	1210	1338
156.6	288	288	3	581	581	645	810	810	901
179.0	327	327	2	327	327	367	610	610	681
Lead Shield									
0.0	203	203	223	516	516	565	291	291	320
22.4	136	136	150	430	430	472	274	274	301
44.8	87	87	97	345	345	378	240	240	263
67.1	47	47	53	268	268	294	206	206	226
89.5	16	16	19	200	200	220	172	172	188
111.9	6	6	1	142	142	156	138	138	151
134.3	19	19	0	92	92	101	103	103	114
156.6	23	23	0	51	51	56	69	69	77
179.0	28	28	0	28	28	31	52	52	58
Outer Steel Shell									
0.0	2786	2786	3058	6439	6436	7053	3408	3408	3742
22.4	1915	1015	2109	5354	5354	5866	3208	3208	3524
44.8	1266	1266	1404	4277	4277	4960	2809	2809	3081
67.1	732	732	822	3314	3314	3637	2409	2409	2644
89.5	312	312	360	2466	2466	2712	2009	2009	2204
111.9	7	7	24	1732	1732	1911	1610	1610	1770
134.3	183	183	7	1114	1114	1232	1210	1210	1338
156.6	259	259	4	609	609	678	810	810	901
179.0	327	327	2	327	327	368	610	610	681

Table B-9-1

Comparison of SCANS Results for Stresses in Bottom End Cap
Generated by a 30 Ft. Drop onto the Cask Bottom (Sample Problem 1)

Primary Impact Angle	Maximum Bending Stress (psi) At Center of End Cap			Maximum Bending Stress (psi) At Edge of End Cap			Maximum Shear Stress (psi) At Edge of End Cap		
	Quasi-static		Dynamic	Quasi-static		Dynamic	Quasi-static		Dynamic
(deg)	Hand Calc	SCANS	SCANS	Hand Calc	SCANS	SCANS	Hand Calc	SCANS	SCANS
0.0	0.0	0.0	-2.4	0.0	0.0	3.8	0.0	0.0	0.6
15.0	630.6	630.6	1380.1	-977.7	-977.7	-2139.7	152.1	152.1	332.8
30.0	1442.4	1442.4	2964.1	-2236.3	-2236.4	-4595.5	347.9	347.9	714.9
45.0	2287.2	2287.2	3257.2	-3546.0	-3546.0	-5049.9	551.6	551.6	785.5
60.0	2969.5	2969.6	3400.4	-4603.9	-4604.0	-5271.9	716.2	716.2	820.1
75.0	3324.2	3324.2	4085.7	-5153.8	-5153.8	-6334.4	801.7	801.7	985.4
90.0	3459.0	3459.0	3855.4	-5362.8	-5362.8	-5977.3	834.2	834.2	929.8
C.G.	3218.5	3218.5	3587.3	-4989.9	-4989.9	-5561.7	776.2	[illegible]6.2	865.2

Table 8-9-2

Comparison of SCANS Results for Stresses in Top End Cap
Generated by a 30 Ft. Drop onto the Cask Bottom (Sample Problem 1)

Primary Impact Angle	Maximum Bending Stress (psi) At Center of End Cap			Maximum Bending Stress (psi) At Edge of End Cap			Maximum Shear Stress (psi) At Edge of End Cap		
	Quasi-static		Dynamic	Quasi-static		Dynamic	Quasi-static		Dynamic
(deg)	Hand Calc	SCANS	SCANS	Hand Calc	SCANS	SCANS	Hand Calc	SCANS	SCANS
0.0	0.0	0.0	0.3	0.0	0.0	0.0	0.0	0.0	0.0
15.0	82.5	82.5	-159.0	0.0	0.0	0.0	7.8	7.8	15.0
30.0	188.7	188.7	-335.4	0.0	0.0	0.0	17.8	17.8	31.7
45.0	299.2	299.2	-401.9	0.0	0.0	0.0	28.3	28.3	38.0
60.0	388.5	388.5	34[illegible].4	0.0	0.0	0.0	36.7	36.7	32.6
75.0	434.9	434.9	443.2	0.0	0.0	0.0	41.1	41.1	41.9
90.0	452.5	452.6	504.4	0.0	0.0	0.0	42.8	42.8	47.7
C.G.	421.0	421.1	469.9	0.0	0.0	0.0	39.8	39.8	44.4

Table B-10-1

Comparison of SCANS Results for Stresses in Bottom End Cap
Generated by a 30 Ft. Drop onto the Cask Top (Sample Problem 1)

Primary Impact Angle	Maximum Bending Stress (psi) At Center of End Cap			Maximum Bending Stress (psi) At Edge of End Cap			Maximum Shear Stress (psi) At Edge of End Cap		
	Quasi-static		Dynamic	Quasi-static		Dynamic	Quasi-static		Dynamic
(deg)	Hand Calc	SCANS	SCANS	Hand Calc	SCANS	SCANS	Hand Calc	SCANS	SCANS
0.0	0.0	0.0	0.1	0.0	0.0	-0.2	0.0	0.0	0.0
15.0	32.3	32.4	-62.4	-50.2	-50.2	96.7	7.8	7.8	15.0
30.0	74.0	74.0	-131.5	-114.7	-114.7	203.9	17.8	17.8	31.7
45.0	117.3	117.3	-157.6	-181.9	-181.9	244.3	28.3	28.3	38.0
60.0	152.3	152.3	135.0	-236.2	- 5.2	-209.4	36.7	36.7	32.6
75.0	170.5	170.5	173.8	-264.4	-264.4	-269.4	41.1	41.1	41.9
90.0	177.4	177.4	197.8	-275.1	-275.1	-306.6	42.8	42.8	47.7
C.G.	165.1	165.1	184.0	-255.9	-256.0	-285.3	39.8	39.8	44.4

Table B-10-2

Comparison of SCANS Results for Stresses in Top End Cap
Generated by a 30 Ft. Drop onto the Cask Top (Sample Problem 1)

Primary Impact Angle	Maximum Bending Stress (psi) At Center of End Cap			Maximum Bending Stress (psi) At Edge of End Cap			Maximum Shear Stress (psi) At Edge of End Cap		
	Quasi-static		Dynamic	Quasi-static		Dynamic	Quasi-static		Dynamic
(deg)	Hand Calc	SCANS	SCANS	Hand Calc	SCANS	SCANS	Hand Calc	SCANS	SCANS
0.0	0.0	0.0	-6.9	0.0	0.0	0.0	0.0	0.0	0.5
15.0	1651.4	1651.4	3613.9	0.0	0.0	0.0	126.6	126.6	277.1
30.0	3777.1	3777.1	7761.7	0.0	0.0	0.0	289.6	289.6	595.1
45.0	5989.1	5989.2	8529.1	0.0	0.0	0.0	459.2	459.2	653.9
60.0	7775.9	7776.0	8904.1	0.0	0.0	0.0	596.2	596.2	682.7
75.0	8704.6	8704.7	10698.7	0.0	0.0	0.0	667.4	667.4	820.3
90.0	9057.6	9057.7	10095.6	0.0	0.0	0.0	694.5	694.5	774.1
C.G.	8427.7	8427.8	9393.7	0.0	0.0	0.0	646.2	646.2	720.2

Table B-11

Comparison of SCANS Results for Tensile and Shear Stresses in Top Closure Bolts Generated by a 30 Ft. Drop onto the Cask botto (Sample Problem 1)

Primary Impact Angle	Maxium Tensile Stress (psi)			Maximum Shear Stress (psi)		
	Quasi-static		Dynamic	Quasi-static		Dynamic
(deg)	Hand Calc	SCANS	SCANS	Hand Calc	SCANS	SCANS
Uniform distribution of tensile stress among all bolts assumed						
0.0	0	0	0	-68124	68124	73240
15.0	0	0	0	-12579	12580	68866
30.0	0	0	0	-9207	9207	25979
45.0	0	0	0	-3524	3524	8885
60.0	0	0	0	3580	3580	3041
75.0	0	0	0	10668	10668	15315
90.0	0	0	0	0	0	0
C.G.	0	0	0	7702	7702	8636
Linear distribution of tensile stress among all bolts assumed						
0.0	0	0	0			
15.0	0	0	0			
30.0	0	0	0			
45.0	0	0	0			
60.0	0	0	0			
75.0	0	0	0			
90.0	0	0	0			
C.G.	0	0	0			

Table 8-12

Comparison of SCANS Results for Tensile and Shear Stresses in Top Closure Bolts Generated by a 30 Ft. Drop onto the Cask Top (Sample Problem 1)

Primary Impact Angle	Maxium Tensile Stress (psi)			Maximum Shear Stress (psi)		
	Quasi-static		Dynamic	Quasi-static		Dynamic
(deg)	Hand Calc	SCANS	SCANS	Hand Calc	SCANS	SCANS
	Uniform distribution of tensile stress among all bolts assumed					
0.0	0	0	0	68124	68124	73240
15.0	13172	13172	28826	55465	55464	57572
30.0	30127	30128	61910	61633	61632	54487
45.0	47771	47772	68031	60580	60578	61303
60.0	62023	62024	71022	51371	51370	62217
75.0	69431	69431	85336	35488	35488	31530
90.0	72247	72247	80526	0	0	0
C.G.	67222	67223	74927	43002	43001	47236
	Linear distribution of tensile stress among all bolts assumed					
0.0	0	0	0			
15.0	17637	17637	38597			
30.0	40340	40340	82895			
45.0	63964	63965	91092			
60.0	83047	83048	95097			
75.0	92966	92967	114263			
90.0	96736	72247	80526			
C.G.	90009	90010	100325			

Table 8-13-1

Comparison of Bending and Shear Stresses for Laminated Endcaps at Impact End
As Obtained in Quasi-static and Dynamic Analyses (Sample Problem 2)

Primary Impact Angle (deg)	Endcap Layer	Maximum Bending Stress (psi): At Center of Cap, Quasi-static, Hand Calc	At Center of Cap, Quasi-static, SCANS	At Center of Cap, Dynamic, SCANS	At Edge Near Cask Cavity Wall, Quasi-static, Hand Calc	At Edge Near Cask Cavity Wall, Quasi-static, SCANS	At Edge Near Cask Cavity Wall, Dynamic, SCANS	Maximum Shear Stress (psi) At Edge Near Cask Cavity Wall: Quasi-static, Hand Calc	Quasi-static, SCANS	Dynamic, SCANS
0.0	Inner	0.0	0.0	-40.5	0.0	0.0	62.8	0.0	0.0	21.4
	Shield							0.0	0.0	1.6
	Outer	0.0	0.0	31.7	0.0	0.0	-49.2	0.0	0.0	21.4
15.0	Inner	-472.3	-472.3	-990.0	732.2	732.2	1534.9	249.0	249.0	522.0
	Shield							19.2	19.2	40.3
	Outer	369.9	369.9	775.4	-573.5	-573.5	-1202.2	249.0	249.0	522.0
30.0	Inner	-1078.4	-1078.4	-2109.3	1672.0	1672.0	3270.2	568.6	568.6	1112.1
	Shield							43.9	43.9	85.8
	Outer	844.6	844.6	1652.0	-1309.5	-1309.5	-2561.2	568.6	568.6	1112.1
45.0	Inner	-1709.0	-1709.0	-2334.9	2649.5	2649.6	3619.9	901.0	901.0	1231.0
	Shield							69.5	69.5	95.0
	Outer	1338.5	1338.5	1828.1	-2075.1	-2075.1	-2835.1	901.0	901.0	1231.0
60.0	Inner	-2218.8	-2218.8	-2516.7	3440.0	3440.0	3901.8	1169.8	1169.9	1326.9
	Shield							90.2	90.2	102.4
	Outer	1737.8	1737.8	1971.1	-2694.2	-2694.2	-3055.9	1169.8	1169.9	1326.9
75.0	Inner	-2484.8	-2484.8	-3021.7	3852.4	3852.4	4684.7	1310.1	1310.1	1593.2
	Shield							101.1	101.1	122.9
	Outer	1946.1	1946.1	2366.6	-3017.2	-3017.2	-3669.1	1310.1	1310.1	1593.2
90.0	Inner	-2585.0	-2585.0	-2882.0	4007.7	4007.8	4468.3	1362.9	1362.9	1519.5
	Shield							105.1	105.1	117.2
	Outer	2024.6	2024.6	2257.2	-3138.9	-3138.9	-3499.6	1362.9	1362.9	1519.5
C.G.	Inner	-2407.3	-2407.3	-2683.9	3732.2	3732.2	4161.1	1269.2	1269.2	1415.1
	Shield							97.9	97.9	109.2
	Outer	1885.4	1885.4	2102.1	-2923.1	-2923.1	-3259.0	1269.2	1269.2	1415.1

Table B-13-2

Comparison of Bending and Shear Stresses for Laminated Endcaps at Free End
As Obtained in Quasi-static and Dynamic Analyses (Sample Problem 2)

		Maximum Bending Stress (psi) At Center of Cap			Maximum Shear Stress (psi) At Edge Near Cask Cavity Wall		
		Quasi-static		Dynamic	Quasi-static		Dynamic
Primary Impact Angle	Endcap Layer	Hand Calc	SCANS	SCANS	Hand Calc	SCANS	SCANS
0.0	Inner	0.0	0.0	74.7	0.0	0.0	1.5
	Shield				0.0	0.0	0.6
	Outer	0.0	0.0	-20.4	0.0	0.0	1.4
15.0	Inner	849.3	849.3	-966.9	17.2	17.2	29.2
	Shield				6.6	6.6	5.3
	Outer	-231.5	-231.5	1611.5	15.4	15.4	38.2
30.0	Inner	1939.2	1939.3	-2067.3	39.3	39.3	62.5
	Shield				15.1	15.1	11.3
	Outer	-528.6	-528.7	3445.5	35.2	35.2	81.6
45.0	Inner	3073.0	3073.1	-2468.7	62.3	62.3	74.6
	Shield				23.9	23.9	13.5
	Outer	-837.6	-837.7	4114.5	55.8	55.8	97.4
60.0	Inner	3989.8	3989.9	3558.7	80.8	80.8	72.1
	Shield				31.1	31.1	27.7
	Outer	-1087.5	-1087.7	-970.1	72.4	72.4	64.6
75.0	Inner	4468.2	4468.3	4591.1	90.5	90.5	93.0
	Shield				34.8	34.8	35.8
	Outer	-1217.9	-1218.1	-1251.5	81.1	81.1	83.3
90.0	Inner	4648.3	4648.5	5184.5	94.2	94.2	105.1
	Shield				36.2	36.2	40.4
	Outer	-1267.0	-1267.2	-1413.3	84.3	84.3	94.1
C.G.	Inner	4328.7	4328.9	4827.9	87.7	87.7	97.8
	Shield				33.7	33.7	37.6
	Outer	-1179.9	-1180.1	-1316.1	78.5	78.5	87.6

NRC FORM 335
(2-89)
NRCM 1102,
3201, 3202

U.S. NUCLEAR REGULATORY COMMISSION

BIBLIOGRAPHIC DATA SHEET

(See instructions on the reverse)

1. REPORT NUMBER *(Assigned by NRC. Add Vol., Supp., Rev., and Addendum Numbers, if any.)*

NUREG/CR-4554
UCID-20674
Vol. 3, Rev. 1

2. TITLE AND SUBTITLE

SCANS (Shipping Cask ANalysis System) A Microcomputer Based Analysis System for Shipping Cask Design Review Theory Manual (Lead Slump in Impact Analysis and Verification of Impact Analysis)

3. DATE REPORT PUBLISHED

MONTH	YEAR
February	1992

4. FIN OR GRANT NUMBER

A0291

5. AUTHOR(S)

R. C. Chun, T. Lo, G. C. Mok, M. C. Witte

6. TYPE OF REPORT

Technical

7. PERIOD COVERED *(Inclusive Dates)*

3/15/89 - 5/31/92

8. PERFORMING ORGANIZATION – NAME AND ADDRESS *(If NRC, provide Division, Office or Region, U.S. Nuclear Regulatory Commission, and mailing address; if contractor, provide name and mailing address.)*

Lawrence Livermore National Laboratory
7000 East Avenue
Livermore, CA 94550

9. SPONSORING ORGANIZATION – NAME AND ADDRESS *(If NRC, type "Same as above"; if contractor, provide NRC Division, Office or Region, U.S. Nuclear Regulatory Commission, and mailing address.)*

Division of Safeguards and Transportation
Office of Nuclear Material Safety and Safeguards
U.S. Nuclear Regulatory Commission
Washington, DC 20555

10. SUPPLEMENTARY NOTES

11. ABSTRACT *(200 words or less)*

A computer system called SCANS (Shipping Cask ANalysis System) has been developed for the staff of the U.S. Nuclear Regulatory Commission to perform confirmatory licensing review analyses. SCANS can handle problems associated with impact, heat transfer, thermal stress, and pressure. A new methodology was developed to allow SCANS to analyze the lead slump behavior of lead-shielded casks during a postulated impact with an unyielding surface.

The methodology is an expansion of the existing lumped-parameter impact analysis method. In the new methodology, it is assumed that the lead and the steel cylinders are not bonded as opposed to the existing bonded-lead assumption. The lead shield is allowed to slide freely relative to the steel cylinders and interact with the steel cylinders only in the radial direction of the shipping cask.

The lead slump methodology described in this revision (Rev 1) of the report is an improved version of the method documented in the original report. The main improvement is in the modeling of the lead behavior. To minimize mathematical difficulty and development cost, the lead was formerly treated as an elastic material with an effective modulus which was tuned to account for the effect of plastic deformation occurring in a cask drop. Although this method gave satisfactory results for 30-ft accident drops, it produced overconservative predictions for 1- to 4-ft normal drops. Thus, the present revision of the method was undertaken to improve the range of applicability of the method. In the improved method described in this report, the lead is treated as an elastic-plastic material and the actual elastic-plastic properties of lead are used instead.

12. KEY WORDS/DESCRIPTORS *(List words or phrases that will assist researchers in locating the report.)*

Shipping Cask
Impact Analysis
Microcomputer Program
Lead Slump

13. AVAILABILITY STATEMENT

Unlimited

14. SECURITY CLASSIFICATION

(This Page)
Unclassified

(This Report)
Unclassified

15. NUMBER OF PAGES

16. PRICE

NRC FORM 335 (2-89)

UNITED STATES
NUCLEAR REGULATORY COMMISSION
WASHINGTON, D.C. 20555

OFFICIAL BUSINESS
PENALTY FOR PRIVATE USE, $300

SPECIAL FOURTH CLASS RATE
POSTAGE & FEES PAID
USNRC
PERMIT No. G-67

[illegible]
US NRC-OADM
DIV FOIA & PUBLICATIONS SVCS
TPS-PDR-NUREG
P-223
WASHINGTON DC 20555

NUREG/CR-4554, Vol. 3, Rev. 1

SCANS (SHIPPING CASK ANALYSIS SYSTEM): A MICROCOMPUTER BASED ANALYSIS SYSTEM FOR SHIPPING CASK DESIGN REVIEW

FEBRUARY 1992